

Introduction

Mucopolysaccharidosis type III

Mucopolysaccharidosis type III belongs to the group of mucopolysaccharidoses, inherited lysosomal diseases due to deficiencies in various enzymes involved in the degradation of cellular glycosaminoglycans (GAG). The glycosaminoglycans themselves are lysosomal degradation products derived by proteolytic removal of the protein core of proteoglycans, the macromolecular forms in which these molecules exist at the cell surface or in the extracellular matrix (Neufeld and Muenzer, 2001).

Mucopolysaccharidosis type III (Sanfilippo syndrome) is an autosomal recessive disorder including four subtypes (Neufeld and Muenzer, 2001). Each is due to deficiency of one of four lysosomal enzymes that participate in the removal of sulfated N-acetylglucosamine residues during the degradation of heparan sulfate: heparan N-sulfatase (EC 3.10.1.1) for A subtype, α -N-acetylglucosaminidase (EC 3.2.1.50) for B subtype, acetyl-CoA: α -glucosaminide acetyltransferase (EC 2.3.1.3.) for C subtype, and N-acetylglucosamine 6-sulfatase (EC 3.1.6.14) for D subtype. Heparan sulfate, that consists of glucuronic acid and L-iduronic acid residues, some of which are sulfated, alternating with α -linked glucosamine residues, is degraded by the action of three glycosidases, three, or perhaps four, sulfatases, and one enzyme that is not a hydrolase but an acetyltransferase as shown schematically in Fig.1. Specifically, iduronate-2-sulfatase removes the sulfate group from the 2-position of L-iduronic acid, and α -L-iduronidase hydrolyzes terminal α -

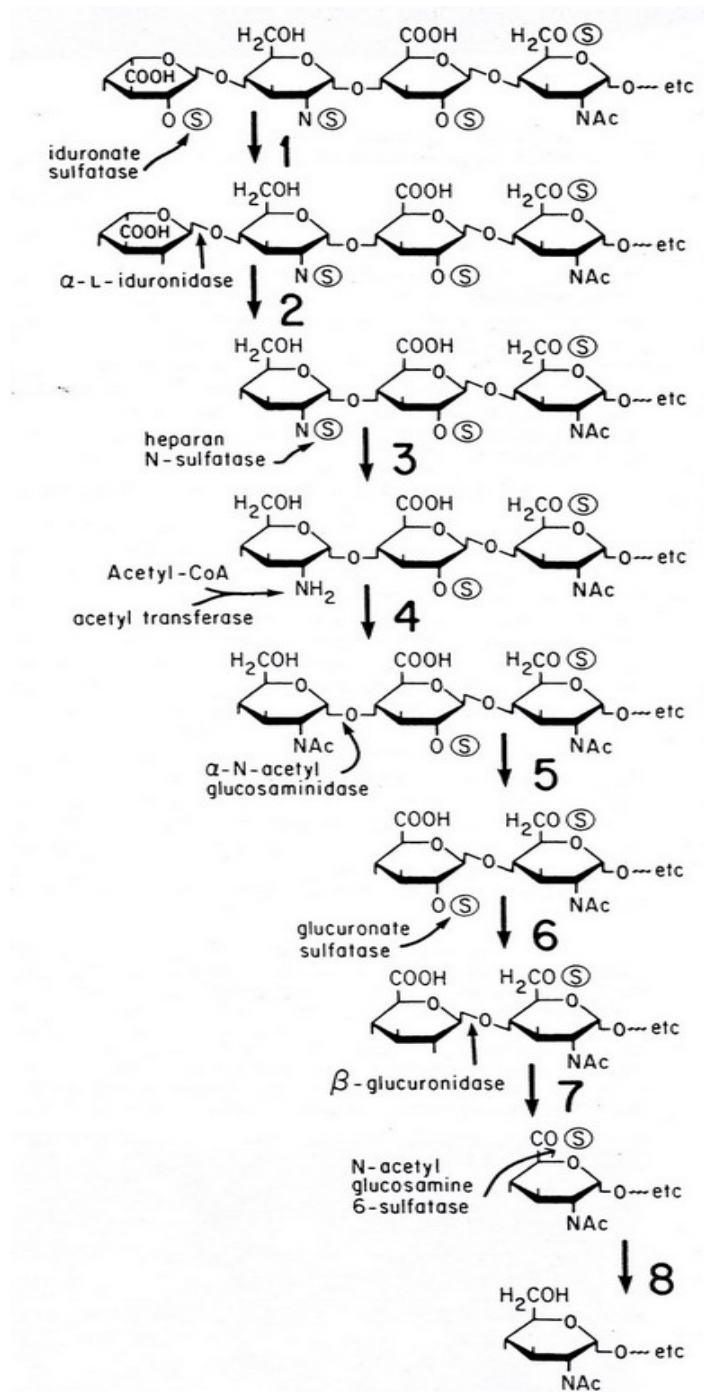


Fig. 1: Stepwise degradation of heparan sulfate.

The deficiency diseases corresponding to the numbered reactions are: 1= MPS II, Hunter syndrome; 2= MPS I, Hunter, Hurler-Scheie, and Scheie syndromes; 3= MPS IIIA, Sanfilippo syndrome type IIIA; 4= MPS IIIC, Sanfilippo syndrome type IIIC; 5=MPS IIIB, Sanfilippo syndrome type IIIB; 6= no deficiency disease yet known; 7= MPS VII, Sly Syndrome; 8=MPS IIID, Sanfilippo syndrome type IIID.

L-iduronic acid residues present in heparan sulfate. In the next step, heparan N-sulfatase is specific for sulfate groups linked to the amino group of glucosamine then acetyl-CoA: α -glucosaminide N-acetyltransferase catalyzes the acetylation of the glucosamine amino groups. The N-acetylglucosamine residues that exist in heparan sulfate or are generated during lysosomal degradation are removed by α -N-acetylglucosaminidase. Enzyme for next step is glucuronate 2-sulfatase that acts on the rare sulfated glucuronic acid residues, then these residues without sulfate group are cleaved by β -glucuronidase. The necessary last enzyme is N-acetylglucosamine 6-sulfatase specific for the 6-sulfated N-acetylglucosamine residues of heparan sulfate. It has been suggested that these enzymes function cooperatively in a complex, allowing the product of one enzyme to be passed efficiently to the next enzyme in the pathway. In the absence of any one of these enzymes, undegraded or partially degraded heparan sulfate accumulates in lysosomes and is also excreted in urine. The Sanfilippo syndromes are rare disorders (1/75,000) that may often remain undiagnosed because of the nonspecific nature of early manifestations. Geographic distribution reported for European populations is uneven, with the A subtype prevalent in the British Isles, the B subtype most common in Southern Europe, and the A, B, and C subtypes distributed in a 3:2:1 ratio in the Netherlands. The biochemistry of these syndromes has been largely studied, but the relationship between molecular mechanisms and clinical signs, particularly behavioral disturbances and neurodegeneration are not yet well understood.

The clinical presentation of MPS III is predominantly characterized by severe central nervous system (CNS) degeneration resulting in progressive mental retardation. The mechanism by which

heparan sulfate storage leads to CNS degeneration is not known (Yogalingam and Hopwood, 2001). It has been proposed that some of the CNS pathology observed in MPS III is due to the lysosomal accumulation of GM2 gangliosides, secondary to heparan sulfate storage. Clinically, the neuropsychiatric abnormalities associated with MPS III can be divided into three phases. Between the ages of one and four years MPS III display development delay alone. The second phase of the illness, which starts in severely affected children at the ages of three to four years and onwards, is associated with severe behavioral disturbances. Affected children are physically quite strong with good mobility under the age of 10 years, making the second phase of the illness the most difficult to manage. The pattern of behavior at this stage of the illness is characterized by frequent and severe temper tantrums, hyperactivity, sleep disturbance, aggression, and a rapid diminution in attention span. During the quieter third and final stage of the illness general physical health and strength deteriorate. Falls are common due to loss of balance. Feeding difficulties are also common due to impaired chewing and swallowing mechanisms. Increasing spasticity combined with degenerative joint disease severely impairs mobility. During this final phase seizures are also common. Death occurs in severely affected children in the mild to late teenage years usually as a result of respiratory infection.

Like most genetic disorders, the clinical phenotype of MPS III varies considerably from severe, to intermediate, to attenuated. In the attenuated form of the disease patients may still be independently mobile at 20-30 years of age. Unlike in most other MPS cases, the somatic features of MPS III, which involve skeletal pathology,

hepatosplenomegaly, and degenerative joint disease, are relatively mild and observed mainly in older patients. Often the lack of somatic involvement combined with the high incidence of false negative results in the urinary screening test for heparan sulfate by some methods leads to difficulty in diagnosing patients with attenuated MPS III.

Mucopolysaccharidosis type IIIB

Mucopolysaccharidosis IIIB (MPS IIIB, Sanfilippo syndrome type B) is inherited as an autosomal recessive disorder caused by mutations in the gene encoding alpha-N-acetylglucosaminidase (NAGLU). Epidemiological data on this disorder and a clear and controlled picture of clinical progression of disease has not been widely studied, but the best estimate of incidence is approximately 1 in every 235,000 live births (Meikle et al.,1999). The disease is characterized, clinically, by profound neurological deterioration, hyperactivity with aggressive behavior, hirsutism, sleep disorders, and mild hepatosplenomegaly. Life span is usually until adolescence, but longer survival occurs among the more mildly affected patients.

NAGLU has been purified from placenta (Weber et al.,1996), liver (Sasaki et al.,1991), and urine (Salvatore et al.,1984); its biosynthesis and maturation has been studied in skin fibroblasts (von Figura et al.,1984) and human carcinoma cells (Di Natale et al.,1985). The reported molecular masses ranged from 80 kDa-86 kDa for the precursor form, 77 kDa for the intermediate form, and 73 kDa for the mature form. The human NAGLU cDNA encodes a 720 aminoacid protein that has six potential N-glycosylation sites at asparagine residues

261, 272, 435, 503, 523, and 532 (Zhao et al., 1995, Zhao et al., 1996; Weber et al., 1996). Recombinant wild type NAGLU has been expressed and characterized in CHO-K1 cells and shown to be synthesized as an 80 kDa precursor polypeptide which is successively cleaved to a 78.5 kDa intermediate polypeptide and a mature 77 kDa polypeptide (Yogalingam et al., 2000). Recombinant NAGLU is secreted from CHO-K1 cells as an 83 kDa precursor and has been used for the generation of polyclonal antiserum (Zhao and Neufeld, 2000; Weber et al., 2001). As most of the other lysosomal enzymes, the NAGLU enzyme is targeted to lysosomes through interaction with the mannose-6-phosphate receptors (MPRs) (Sahajian et al., 1981; Dahms et al., 1989). The phosphorylated lysosomal enzymes bind to MPRs that are located in the membrane of the clathrin-coated vesicles budding from the trans-Golgi network. These vesicles then fuse with other acidic vesicles (such as late endosomes) leading, in acid condition, to the dissociation of the lysosomal enzymes into the lumen, while the receptors recycle back to the Golgi. Mannose-6-phosphate receptors are also present on the plasma membrane, where they are able to bind circulating or extracellular lysosomal enzymes and deliver them to the lysosomes. Two different MPRs have been identified, characterized, and their cDNAs cloned. The first MPR to be characterized, identified as CI MPR, or MPR 300, or Man-6-P/IGF, is a membrane-associated glycoprotein that binds ligand independent of divalent cation; by biochemical studies has been confirmed that sequence of insulin like growth factor II (IGF-II) receptor corresponds to that of the CI-MPR. The second mannose-6-phosphate receptor, cation dependent receptor (CD-MPR), or MPR46, is also a membrane-associated glycoprotein but requires divalent cations for optimal ligand

binding. Lysosomal enzymes are also partially secreted in the extracellular environment from which thus can be reinternalized by binding with the cation-independent MPR (CI MPR). In contrast to other lysosomal hydrolases, recombinant NAGLU produced in Chinese hamster ovary (CHO) cells is not efficiently captured by MPS IIIB cells, both in vitro (Zhao and Neufeld, 2000; Weber et al.,2001) and in vivo (Yu et al.,2000).

The gene locus for NAGLU has been localized to chromosome 17q21 (Fig.2). The 3' end of the NAGLU gene resides in the upstream flanking region of the 17- β -hydroxysteroid dehydrogenase gene. The NAGLU gene, interrupted by five introns, is 8.2 kb long from translation start site to polyadenylation site. The first exon is indicated provisionally as containing an additional 0.3 kb of untranslated sequence, based on primer extension studies that showed an apparent transcription start site 332 and 321 nucleotides upstream of the initiating methionine. But because that region contains neither TATA box nor SP1 sites and is not particularly G + C rich, the untranslated region may extend even further upstream (Zhao et al., 1996). The knowledge of the gene allowed mutation analysis in affected patients.

MPS IIIB shows extensive molecular heterogeneity with more than 100 different mutations identified to date including: 73 nonsense/missense mutations, 18 deletions, 14 insertions, and 2 splicing mutations (<http://www.hgmd.cf.ac.uk/>). All mutations occur once or at relatively low frequencies; most of these alterations are reviewed by Yogalingam and Hopwood (2001; Tab.1). Of the eight nonsense mutations all are associated with severe phenotypes; among these mutations, R297X occurred at the highest frequency (11.5%) in MPS

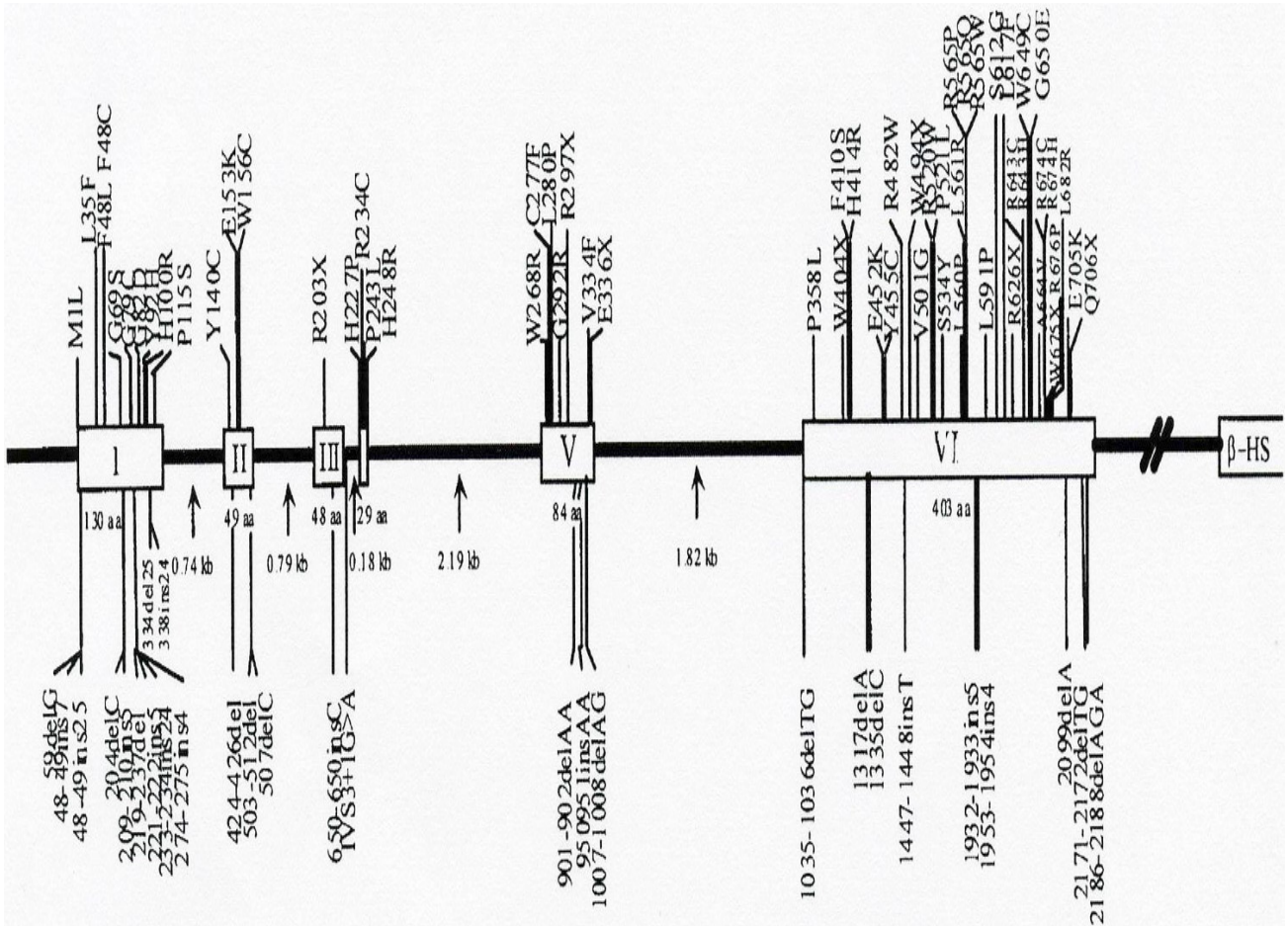


Fig. 2: Location of MPS IIIB mutations in the NAGLU gene.

Exons are represented by boxes and exon numbers are indicated in roman numerals. The position of missense and nonsense mutations are shown above the gene. Other mutations (insertions, deletions, and a splice site mutation) are show below the gene.

**Table 1. Mutations in the NAGLU gene causing MPS IIIB
(from Yogalingam and Hopwood, 2001)**

| Mutation | Base change | Effect | Country | 2nd allele | Phenotype | Reference |
|---------------------|---------------------------|---|--------------------|------------|------------|---------------------------|
| MIL | 1A>T | Initiation codon removed with no other initiation site near | DE | C277F | N.R. | Bunge et al. [1999] |
| 48-49ins GGGGCCG | Duplication of nt 49-55 | f.s. termination at pos 121 | AU | 2099delA | Severe | Weber et al. [1999] |
| 48-49ins25 | Duplication of nt49-74 | f.s. termination at pos. 121 | AU | 1317delA | Severe | Weber et al. [1999] |
| 59delG | | f.s. premature termination at pos 121 after 101 altered aa | AU | R626X | Severe | Weber et al. [1999] |
| L35F | 103C>T | Conservative aa exchange | IT | G292R | Severe | Tessitore et al. [2000] |
| F48C | 143T>G | Non-conservative aa exchange | PK | F48C | Severe | Beesley et al. [1998] |
| F48L | 144C>G | Conservative aa exchange | AU | R297X | Attenuated | Weber et al. [1999] |
| 204delC | | f.s. premature termination at pos 121 after 52 altered aa | IT | N.I. | Severe | Tessitore et al. [2000] |
| G69S | 205G>A | Non-conservative aa exchange | AU | R297X | Attenuated | Weber et al. [1999] |
| 209-210ins GCGGC | Duplication of nt 210-214 | Direct repeat of bp 210-214, f.s. termination at pos 121 | NL | R297X | Severe | Weber et al. [1999] |
| G79C | 235G>T | Non-conservative aa exchange | TR | G79C | N.R. | Bunge et al. [1999] |
| 219-237del | | f.s. premature termination after 41 altered aa | UK | Y140C | Severe | Beesley et al. [1998] |
| 221-222ins GCGCG | | f.s. premature termination at pos 122 after 49 altered aa | IT | N.I. | N.R. | Tessitore et al. [2000] |
| 233-234 ins24 | Duplication of nt 233-241 | In-frame duplication of 24 bp at pos 233, 8 aa insertion | US | S612G | Attenuated | Zhao et al. [1998] |
| 274-275 insCTGC | | f.s. premature termination after 132 altered aa | DE | R565Q | N.R. | Bunge et al. [1999] |
| G82D | 245G>A | Non-conservative aa exchange | IT | G82D | N.R. | Tessitore et al. [2000] |
| Y92H | 274T>C | Non-conservative aa exchange | IT | Y140C | N.R. | Schmidtchen et al. [1998] |
| H100R | 299A>G | Conservative aa exchange | IR | H100R | N.R. | Bunge et al. [1999] |
| 334-358del | | f.s. premature termination after 1 altered aa | GR | 334-358del | Severe | Beesley et al. [1998] |
| 338-339 ins24 | Duplication of nt 315-338 | In-frame duplication of aa 72-79 | TR | R565Q | N.R. | Bunge et al. [1999] |
| P115S | 343C>T | Non-conservative aa exchange | IT | P115S | N.R. | Schmidtchen et al. [1998] |
| Y140C | 419A>G | Non-conservative aa exchange | IT | Y92H | N.R. | Schmidtchen et al. [1998] |
| | | | CZ | W404X | N.R. | Bunge et al. [1999] |
| | | | GR | R626X | Severe | Beesley et al. [1998] |
| | | | GM | L682R | N.R. | Schmidtchen et al. [1998] |
| | | | 00737 ^a | | | |
| | | | US | R674C | Severe | Zhao et al. [1998] |
| 424-426del | | In-frame deletion of codon 142 | DE | N.I. | N.R. | Bunge et al. [1999] |
| E513K | 457G>A | Non-conservative aa exchange | GM | E153K | N.R. | Schmidtchen et al. [1998] |
| | | | 01426 ^a | | | |
| W156C | 468G>T | Non-conservative aa exchange | IT | Y140C | Severe | Tessitore et al. [2000] |
| 503-512del | | f.s. premature termination at pos 184 after 13 altered aa | US | 503-512del | N.R. | Zhao et al. [1996] |
| | | | AU | H414R | Severe | Weber et al. [1999] |
| 507delC | | f.s. premature termination at pos 184 after 15 altered aa | IT | N.I. | N.R. | Tessitore et al. [2000] |
| R203X | 607C>T | Chain termination at codon 203 | ET | A664V | N.R. | Schmidtchen et al. [1998] |
| 650-651 insC | | f.s. termination after 14 altered aa | IT | P115S | N.R. | Schmidtchen et al. [1998] |
| IVS3+ 1G>A | G>A | Destroys the 5' splice donor of intron 3 | IT | N.I. | Severe | Tessitore et al. [2000] |
| H227P | 680A>C | Non-conservative aa exchange | AU | P521L | Attenuated | Weber et al. [1999] |
| R234C | 700C>T | Non-conservative aa exchange | SP | R234C | Severe | Beesley et al. [1998] |
| H248R | 743A>G | Conservative aa exchange | NL | N.I. | Attenuated | Weber et al. [1999] |
| W268R | 802T>C | Non-conservative aa exchange | PK | W268R | Severe | Beesley et al. [1998] |
| C277F | 830G>T | Non-conservative aa exchange | DE | MIL | N.R. | Bunge et al. [1999] |
| L280 | 839T>C | Non-conservative aa exchange | PL | N.I. | N.R. | Bunge et al. [1999] |

(continued)

Table 1. Continued.

| Mutation | Base change | Effect | Country | 2nd allele | Phenotype | Reference |
|-----------------|-------------|---|---------|--------------------|------------|---------------------------|
| G292R | 874G>A | Non-conservative aa exchange | IR | G292R | N.R. | Bunge et al. [1999] |
| | | | AU | R565W | Severe | Weber et al. [1999] |
| R297X | 889C>T | Chain termination at codon 297 | AU | F48L | Attenuated | Weber et al. [1999] |
| | | | AU | G69S | Attenuated | Weber et al. [1999] |
| | | | US | R297X | Severe | Zhao et al. [1998] |
| | | | NL | R297X | Severe | Weber et al. [1999] |
| | | | UK | L591P | Severe | Beesley et al. [1998] |
| | | | GM | R643H | N.R. | Zhao et al. [1996] |
| | | | | 02552 ^a | | |
| | | | NL | R676P | Severe | Weber et al. [1998] |
| | | | UK | E705K | Severe | Beesley et al. [1998] |
| | | | NL | 209-210 | Severe | Weber et al. [1999] |
| | | | | insGCGGC | | |
| | | | EE | 1932-1933 | Severe | Beesley et al. [1998] |
| | | | | insGCTAC | | |
| | | | AU | 2171-2172 | Severe | Weber et al. [1999] |
| | | | | delTG | | |
| 901-902 delAA | | f.s. termination after 55 altered aa | IT | 901-902 delAA | N.R. | Schmidtchen et al. [1998] |
| 950-951 ins AA | | f.s. termination at pos 338 after 22 altered aa | AU | N.I. | Severe | Weber et al. [1999] |
| V334F | 1000G>T | Conservative aa exchange | AU | V334F | Severe | Weber et al. [1999] |
| E336X | 1006G>T | Chain termination at codon 336 | IT | E336X | Severe | Tessitore et al. [2000] |
| 1007-1008 delAG | | f.s. premature termination after 14 altered aa | DE | N.I. | N.R. | Bunge et al. [1999] |
| 1035-1036 delTG | | f.s. termination at pos 386 after 38 altered aa | AU | R565P | Severe | Weber et al. [1999] |
| P358L | 1073C>T | Non-conservative aa exchange | GM | P358L | N.R. | Schmidtchen et al. [1998] |
| | | | | 02931 ^a | | |
| W404X | 1211G>A | Chain termination at codon 404 | CZ | Y140C | N.R. | Bunge et al. [1999] |
| | | | US | W404X | Severe | Weber et al. [1999] |
| F410S | 1229T>C | Non-conservative aa exchange | AU | N.I. | Severe | Weber et al. [1999] |
| H414R | 1241A>G | Conservative aa exchange | AU | 503-512 del | Severe | Weber et al. [1999] |
| 1317delA | | f.s. termination at pos 474 after 35 altered aa | AU | 48-49 ins25 | Severe | Weber et al. [1999] |
| 1335delC | | f.s. termination after 29 altered aa | PK | 1335delC | Severe | Beesley et al. [1998] |
| E452K | 1354G>A | Non-conservative aa exchange | TR | E452K | N.R. | Bunge et al. [1999] |
| Y455C | 1364A>G | Non-conservative aa exchange | US | P521L | Severe | Zhao et al. [1998] |
| | | | US | R674H | N.R. | Zhao et al. [1998] |
| R482W | 1444C>T | Non-conservative aa exchange | TR | R482W | N.R. | Bunge et al. [1999] |
| 1447-1448 insT | | f.s. termination after 32 altered aa | UK | R565W | Severe | Beesley et al. [1998] |
| W494X | 1482G>A | Chain termination at codon 494 | NO | W494X | Severe | Weber et al. [1999] |
| V501G | 1502T>G | Non-conservative aa exchange | IT | V501G | Severe | Tessitore et al. [2000] |
| R520W | 1558C>T | Non-conservative aa exchange | IT | N.I. | Severe | Tessitore et al. [2000] |
| P521L | 1562C>T | Non-conservative aa exchange | AU | H227P | Attenuated | Weber et al. [1999] |
| | | | US | Y455C | Severe | Zhao et al. [1998] |
| | | | AU | P521L | Severe | Weber et al. [1999] |
| | | | UK | P521L | Severe | Beesley et al. [1998] |
| S534Y | 1601C>A | Non-conservative aa exchange | IT | N.I. | Attenuated | Tessitore et al. [2000] |
| L560P | 1679T>C | Non-conservative aa exchange | AU | N.I. | Attenuated | Weber et al. [1999] |
| L561R | 1682T>G | Non-conservative aa exchange | BG | L561R | N.R. | Bunge et al. [1999] |
| R565W | 1693C>T | Non-conservative aa exchange | UK | 1447-1448 insT | Severe | Beesley et al. [1998] |
| | | | AU | G292R | Severe | Weber et al. [1999] |
| R565Q | 1694G>A | Non-conservative aa exchange | DE | 274-275 | N.R. | Bunge et al. [1999] |
| | | | | insCTGC | | |
| | | | TR | 338-339 | N.R. | Bunge et al. [1999] |
| | | | | ins25 | | |
| R565P | 1694G>C | Non-conservative aa exchange | AU | 1035del2 | Severe | Weber et al. [1999] |
| L591P | 1772T>C | Non-conservative aa exchange | UK | R297X | Severe | Beesley et al. [1998] |
| S612G | 1834A>G | Non-conservative aa exchange | US | 233-234 ins24 | Attenuated | Zhao et al. [1998] |

Table 1. Continued

| Mutation | Base change | Effect | Country | 2nd allele | Phenotype | Reference |
|-----------------------|-------------|--|--|---|--|---|
| L617F | 1851G>C | Conservative aa exchange | AU | N.I. | Severe | Weber et al. [1999] |
| R626X | 1876C>T | Chain termination at codon 626 | AU GM 00156 ^a UK AU | 59delG R626X R626X | Severe N.R. Severe Severe | Weber et al. [1999] Zhao et al. [1996] Beesley et al. [1998] Weber et al. [1999] |
| R643C | 1927C>T | Non-conservative aa exchange | NL | R643C | Attenuated | Weber et al. [1999] |
| R643H | 1928G>A | Conservative aa exchange | GM 02552 ^a | R297X | N.R. | Zhao et al. [1996] |
| 1932-1933 insGCTAC | | f.s. termination after 3 altered aa | EE | R297X | Severe | Beesley et al. [1998] |
| W649C | 1947G>C | Non-conservative aa exchange | IT | W649C | Severe | Tessitore et al. [2000] |
| G650E | 1949G>A | Non-conservative aa exchange | AU | R674C | Severe | Weber et al. [1999] |
| 1953-1954 insGCCA | | f.s. termination after 33 altered aa | IT | N.I. | Severe | Tessitore et al. [2000] |
| A664V | 1991C>T | Conservative aa exchange | ET | R203X | N.R. | Schmidtchen et al. [1998] |
| R674C | 2020C>T | Non-conservative aa exchange | US | Y140C | Severe | Zhao et al. [1998] |
| R674H | 2021G>A | Conservative aa exchange | US US N.R. TR US US | R674H R674 R674H R674H Y455C Q706X | Severe Severe N.R. N.R. N.R. Severe | Zhao et al. [1998] Zhao et al. [1998] Zhao et al. [1998] Zhao et al. [1996] Bunge et al. [1999] Zhao et al. [1998] Zhao et al. [1998] |
| W675X | 2024G>A | Chain termination at codon 675 | US | Q706X | Severe | Zhao et al. [1998] |
| R676P | 2027G>C | Non-conservative aa exchange | NL | R297X | Severe | Weber et al. [1999] |
| L682R | 2045T>G | Non-conservative aa exchange | GM 00737 ^a | Y140C | N.R. | Schmidtchen et al. [1998] |
| 2099 delA | | f.s. termination at pos 823; 44 altered and 80 additional aa | UK | 2099delA | Severe | Beesley et al. [1998] |
| E705K | 2113G>A | Non-conservative aa exchange | UK | R297X | Severe | Beesley et al. [1998] |
| Q706X | 2116C>T | Chain termination at codon 706 | US | W675 | Severe | Zhao et al. [1998] |
| 2171-2172 delTG | | f.s. termination at pos 786; 19 altered and 43 additional aa | AU | R297X | Severe | Weber et al. [1999] |
| 2186-2188 delAGA | | In frame deletion of codon 729 | IT | N.I. | Severe | Tessitore et al. [2000] |

IIIB patients. This mutation has been engineered into the wild type NAGLU cDNA and expressed in CHO-K1 cells: only a 34 kDa truncated polypeptide with a rapid degradation was observed. Also the E336X nonsense mutation has been expressed in COS cells: it was detected as inactive, truncated polypeptides which remained stable over a 24 h period (Tessitore et al.,2000). Yogalingam and Hopwood reported also 50 missense mutations in the NAGLU gene, most of these are unique mutations. However, some of them resulted to be recurrent: Y140C has been detected in eight out of 148 (5.4%) reported MPS IIIB alleles. R674H, R643C, R565W, and P521L occur in MPS IIIB patients at frequencies of 4.7%, 3.4%, 3.4%, and 4.1% respectively. As expected, the mutations which are reported to be associated with attenuated clinical phenotypes and therefore to maintain some residual activity, are all missense mutations. Some of these were deeply studied: for example, F48L has been engineered into the wild type NAGLU cDNA and expressed (Yogalingam et al.,2000). When over-expressed in MPS IIIB skin fibroblast via retroviral mediated gene transfer, F48L NAGLU activity corresponded to 3.8% of NAGLU activity levels found in wild type NAGLU transduced MPS IIIB fibroblasts. Concerning splicing mutations, IVS3+1G>A, for example, disrupts the consensus sequence between exon 3 and intron 3 (Tessitore et al.,2000). For this alteration the deletion of both exons 2 and 3, which disrupts the reading frame, resulted in no detectable NAGLU protein when expressed in COS cells. Sixteen deletions and eleven insertions have also been identified in the NAGLU gene, these mutations are associated with severe Sanfilippo phenotypes presumably due to increased instability and/or lack of residual activity. Many of these alterations cause a change in the reading frame resulting in

the addition of altered aminoacid and/or premature chain termination. Interpretation of the clinical phenotype resulting from different mutations is very difficult for a disorder where the predominant feature is CNS degeneration; the prediction of genotype-phenotype correlation is very difficult for MPS IIIB as for all the MPS. In addition, this correlation for MPS IIIB is also complicated by the presence of polymorphisms such as the missense change G737R (Yogalingam and Hopwood, 2001).

Animal models for MPS III

Animal models represent a powerful tool to assess the biological pathways and pathological mechanism of a disease condition. However, the limitation for the use of naturally occurring large animal models has been their limited availability, difficult and costly maintenance, and in some cases the lack of resemblance to the corresponding human disease. In contrast, the laboratory mouse offers multiple advantages as an experimental system. Mice are small and relatively inexpensive to maintain, have short life span and gestation period, and produce abundant offspring, allowing the timely generation of large experimental groups for analysis. In addition, creation of inbred strains of mice is feasible eliminating the variability of a spurious genetic background, thereby facilitating the interpretation of the results. In general, the mouse shares biochemical pathways and developmental stages with larger mammals including humans, and its genomic organization is relatively conserved compared to humans (Sabatini et al 2001). Because of this similarity, the generation of mutant mouse strains by gene targeting technology in

embryonic stem (ES) cells has contributed greatly to the understanding of biochemical pathways, protein function and pathological mechanism of disorder observed in humans (Sabatini et al, 2001).

To date, animal models have been reported for all forms of MPS III except type IIIC; a caprine form of Sanfilippo type D result from a nonsense mutation and consequent deficiency of lysosomal N-acetylglucosamine 6-sulfatase (G6S) activity and are associated with tissue storage and urinary excretion of heparan sulfate. Using special stains, immunohistochemistry, and electron microscopy, secondary lysosomes filled with GAG were identified in most tissue from affected goats. Primary neuronal accumulation of heparan sulfate and secondary storage of gangliosides were observed in the CNS of these animals. In addition, morphological changes in the CNS such as neuritic expansions and other neuronal alterations that may have functional significance were also seen. The spectrum of lesions was greater in the severe form of caprine MPS IIID and included mild cartilaginous bony, and corneal lesions. The most pronounced neurological deficits in the severe form were partly related to a greater extent of CNS dysmyelination (Jones et al., 1998).

Two cases of MPS IIIA have been reported in adult wire-haired Dachshund littermates (Fischer et al.,1998). Clinical and pathologic features paralleled the human disorder; both dogs exhibited progressive neurologic disease without apparent somatic involvement. Pelvic limb ataxia was observed when the dogs were 3 years old and progressed gradually within 1-2 years to severe generalized spinocerebellar ataxia. Mentation remained normal throughout the course of the disease. A mucopolysaccharide storage disorder was indicated in both dogs by

positive toluidine blue spot tests of urine. The diagnosis of MPS IIIA was confirmed by documentation of urinary excretion and tissue accumulation of heparan sulfate and decreased sulfamidase activity in fibroblasts and hepatic tissue. Mild cerebral cortical atrophy and dilation of the lateral ventricles were grossly evident in both dogs. Light microscopically, fibroblasts, hepatocytes, and renal tubular epithelial cells were vacuolated. Within the nervous system, cerebellar Purkinje cells, neurons of brainstem nuclei, ventral and dorsal horns, and dorsal ganglia were distended with brightly autofluorescent. Neuronal storage appeared as membranous concentric whorls, lamellated parallel membrane stacks, or electron-dense lipid globules. (Fischer et al., 1998). In the 1999 was described a spontaneous mouse mutant that replicates many of the features found in MPS IIIA children (Bhaumik et al., 1999). Brain sections revealed neurons with distended lysosomes filled with membranous and floccular materials with some having a classical zebra body morphology. Affected mice usually died at 7-10 months of age exhibiting a distended bladder and hepatosplenomegaly. Enzyme assay of liver and brain extracts revealed a dramatic reduction in sulfamidase activity. Other lysosomal hydrolases that degrade heparan sulfate or other glycans and glycosaminoglycans were either normal, or were somewhat increased in specific activity.

To date, three animal models have been described for MPS IIIB: two spontaneous models in the emu and in the dog and the knockout mouse.

In *Dromaius novaehollandiae* (emu), was described a progressive neurologic disease characterized by NAGLU deficiency and heparan accumulation (Giger et al., 1997). In the first months of life, affected birds

develop ataxia, tremor, circling, lethargy, and inappetence; death ensues by 6 months of age. Both parents of affected birds had intermediate levels of NAGLU activity, thus suggesting an autosomal recessive mode of inheritance. Liver had elevated levels of enzymes involved in glycosaminoglycan metabolism, while other lysosomal enzymes were within the normal range. These findings indicated that affected emus had an avian lysosomal disease homologous to the human disorder Sanfilippo syndrome type B. To define the molecular basis, the sequences of the normal emu NAGLU cDNA and gene were determined by PCR based approaches using primers for highly conserved regions of evolutionarily distant NAGLU homologues. The exon-intron structure of the emu NAGLU gene is similar to that of mouse and human; however, the introns are much shorter than those in the human and mouse NAGLU genes. The emu NAGLU gene appears to be highly polymorphic, with 19 variations found in the coding region alone.

Between animals models for MPS IIIB, the canine model is unique in that it is a large mammalian model with a clear and overt neurological phenotype (Ellinwood et al.,2003). Clinically the canine model is characterized as an early adult onset cerebellar ataxia. The disease was initially described in the Schipperke breed, where onset of clinical signs were seen at 18-24 months of age. Disease progression lasted from 1-2 years, upon which owners elected euthanasia. Biochemically and histopathologically, the model is characterized by lysosomal distention and granules or vacuoles in neuron, microglia, and perithelial cells throughout the CNS. There is almost a complete loss of Purkinje cells in the terminal stages of the canine model. The storage of GM2 ganglioside is apparent as early as a few months of age. Storage in peripheral tissues

is most severe in the liver and kidney, where distal convoluted tubules are most affected. Storage in other tissues is confined primarily to resident macrophages.

The mouse model of MPS IIIB has been produced by the disruption of exon 6 in the murine NAGLU gene (Li et al., 1999). After enzymatic digestion a 852-bp fragment within exon 6 was replaced by a cassette containing the neo^r gene under control of the phosphoglycerate kinase promoter. Mutant mice are healthy and fertile while young and could survive for 8-12 months. They are totally deficient in α -N-acetylglucosaminidase and have massive accumulation of heparan sulfate in liver and kidney as well as secondary changes in activity of several other lysosomal enzymes in liver and brain and elevation of gangliosides G_{M2} and G_{M3} in brain. Vacuolation was seen in many cells, including macrophages, epithelial cells, and neurons, and became more prominent with age. Although most vacuoles contained finely granular material characteristic of glycosaminoglycan accumulation, large pleiomorphic inclusions were seen in some neurons and pericytes in the brain. The hyperactivity that is characteristic of affected children was not observed even in younger mice. No therapy is available for the affected MPS IIIB patients and the rarity of this disorder makes the use of this model critical for studies of pathogenesis and development of therapies particularly enzyme replacement therapy (Yu et al., 2000) and gene therapy (Fu et al., 2002; Cressant et al., 2004; Di Natale et al., 2005).

Pathogenesis studies on MPS IIIB

The pathogenesis of MPS IIIB is not well understood, as for the other lysosomal diseases; however, few studies have been performed on the mouse model (Li et al.,2002; Ohmi et al.,2003). The first report (Li et al.,2002) showed the effects of possible heparan sulfate accumulation on neuroplasticity that are within the spectrum of action of fibroblast growth factor and their receptors (Li et al., 2002). Heparan sulfate has functions important for development and plasticity for neural cells (Ruoslahti and Yamaguchi,1991; Brickman et al.,1998), is known to be a low-affinity receptor for members of the FGF family, such as FGF-1 and FGF-2 (Yayon et al.,1991; Nurcombe et al.,1993; Rahmoune et al.,1998); one of the key functions of the FGF-2/HS complex is to regulate astrocyte proliferation and function (Gomez-Pinilla et al., 1995). Astrocytes have a critical role in maintaining brain homeostasis (Ridet et al., 1997), particularly after insult or disease (Hatten et al., 1991; Acarin et al., 2000). For example, astrocytes maintain ionic equilibrium and detoxify the extracellular environment (Rothstein et al., 1996). They also produce cytokines and growth factors, including FGFs. Astrocyte malfunction during periods of physiological demand, such as after injury or disease, may compromise neuronal vitality and brain function. Autopsy studies on brains of MPS III patients have shown an increased number of reactive astrocytes (Tamagawa et al., 1985; Kurihara et al., 1996). There was an overall increase in the relative density of reactive astrocytes in the affected mice brains, but these astrocytes showed a reduced capacity to react to injury. The progressive increase of reactive astrocytes over time suggests that a possible chronic accumulation of HS may be responsible

for astrocyte activation/proliferation. This finding parallels the observations of above-normal reactive astrocyte density in MPS IIIB patients. In a subsequent study, the involvement of microglia in brain pathology of the affected MPS IIIB mice was evidenced (Ohmi et al.,2003). Microglia have been implicated in the pathogenesis of a number of neurodegenerative conditions, including Alzheimer's disease, HIV dementia, and multiple sclerosis. Microglia cells are ubiquitously distributed in the central nervous system and comprise up to 20% of the total glial cell population in brain. These cells are related to monocytes and macrophages (Lee et al.,2001). As the primary immune effector cells in the central nervous system, microglia cells migrate to the site of tissue injury or inflammation, where they respond to invading pathogens or other inflammatory signals. Like monocytes/macrophages, they also secrete inflammatory cytokines and toxic mediators, which may amplify the inflammatory responses (Minghetti et al.,1998; Gonzalez-Scarano et al.,1999). Microglia cells and astrocytes underwent apoptosis upon inflammatory activation, and nitric oxide acted as an autocrine cytotoxic mediator in this process (Lee et al., 2001; Suk et al., 2001). Activation of glial cells may be intended to protect neurons at first. More frequently, however, activation of glia cells and inflammatory products derived from them have been implicated in neuronal destruction commonly observed in various neurodegenerative diseases (Gonzalez-Scarano et al., 1999). Among the various cytotoxic factors released by activated microglia, reactive oxygen species (ROS) such as superoxide free radical appear to play a key role in the inflammation-mediated oxidative damage to neurons. Growing evidence suggests that the generation of oxidants does not result simply from an accidental disruption of aerobic metabolism,

but rather from an active process crucial for non-specific immune defenses of the brain. While essential for survival, these processes may be inappropriately activated to cause neurodegeneration. Oxidants can be produced by essentially all of the cells in the brain. For example, NADPH oxidase, the super-oxide-generating enzyme in phagocytes, is expressed not only by microglia but also by astrocytes and neurons (Hischiropoulos et al., 2003).

Multiple lines of evidence demonstrate that oxidative stress is an early event in pathologies as Alzheimer's disease (AD) (Zhu et al., 2004). Over the past decade, modification to virtually all classes of biomacromolecules indicative of oxidative stress has been described in association with susceptible neurons of AD; (1) DNA and RNA oxidation, DNA repair deficiency is also noted in AD since higher levels of DNA breaks, DNA nicking and fragmentation are observed in AD patients (Mecocci et al., 1994); (2) Oxidative modification of proteins, some specifically oxidized proteins have recently been identified by proteomics and it is notable that many are either enzymes that are related to ATP generation or enzyme involved in glycolysis. Therefore, oxidative modification may lead to metabolic impairment in AD, moreover crosslinking of proteins, by oxidative processes, may lead to the resistance of the lesions to intracellular and extracellular removal even though they are extensively ubiquitinated and this resistance of neurofibrillary tangles to proteolysis might play an important role in the progression of AD; (3) Lipid peroxidation that lead to eventual cell death, and (4) Modification to sugars that is marked by increased glycation and glycooxidation.

An excellent example to discuss the significance of oxidative processes as a central but not an initiating event for the development of clinical disease is Parkinson disease, where the dopaminergic neurons in the substantia nigra are selectively injured. Genetic factors or environmental toxins that epidemiological studies have shown to be risk factors are capable of generating reactive intermediates, directly alkylating reduced thiols inhibiting complex I of the mitochondrial transport chain, inducing α -synuclein aggregation, and activating microglia. Possibly, they may also alter iron or other divalent metal homeostasis as well as dopamine metabolism, permitting an increase in non-vesicle associated dopamine levels. All these events permit formation of reactive oxygen and nitrogen intermediates that propagate cellular dysfunction, leading to cell death (Hischiropoulos et al.,2003).

Aim of the research project

During the first two years of the Ph.D. course (2003-2004) I collaborated to a study on the murine model of MPS IIIB, based on gene therapy mediated by a third generation lentiviral-NAGLU vector showing its therapeutic potential and limits (Di Natale et al.,2005).

This thesis refers to the experimental work performed in the last two years of the Ph.D. course (2005-2006). I studied MPS IIIB-specific gene expression profiles in brain and cerebellum of affected mice by cDNA microarray analysis and Real Time PCR, trying to understand the pathogenesis of this devastating disease.

Experimental work

Materials and methods

Animals

The mouse model of MPS IIIB was created by targeted disruption of exon 6 of the corresponding mouse NAGLU gene Li et al. (1999). The biochemical phenotype of mutant mice is generally similar to that of the human disorder, the only exception being that affected mice do not show increased urinary excretion of heparan sulfate. The mice were genotyped by polymerase reaction analysis performed on DNA sample extracted from tail clipping exactly 1 month after birth. PCR_s were performed in a total volume of 100 µl containing 500ng of template DNA extracted from tail clipping, 1xPCR buffer from PerkinElmer, 0.2 µM of each dNTP, 2.5 units of *Taq* polymerase and two sets of the following primers (0.5 µM each): (i) MXXDe1F, sense primer starting at position 6773 of the murine NAGLU gene, GenBank[®] accession number AF003255 (5'-GCTCCTACTCAGAAGTGTCTACAACCTGCTC-3'), and MXXDe1R, antisense primer starting at position 7279 (5'-GAGGCTGGTAGTAATCAGCCACCAGTCCTG-3'). Amplification yielded a 537 bp fragment in the presence of the normal allele, no band in the presence of the mutant allele; (ii) Neo1F, sense primer starting at position 202 in the Neo ORF (5'-GTGGCTGGCCACGACGGGCGTTCCTTGCG-3'), and M7R, antisense primer starting at position 7454 of the murine NAGLU gene (5'-GAGGAAGATCTTCTTGGAGAGGTCCACGGTG-3'). Amplification yielded no band in the presence of the normal allele but yielded a 1200 bp band in the presence of the mutant allele. Cycling

conditions were the following: 96°C for 5 min, 35 cycles at 95°C for 45 s, 64°C for 35 s and 72°C for 2 min.

Antibodies, chemicals and statistical analysis

The primary rabbit polyclonal antibody against Caspase-11 was from Oncogene research products; primary polyclonal goat anti-gp91^{phox} and rabbit anti-BDNF antibodies were from Santa Cruz Biotechnology. The biotinylated anti-rabbit secondary antibody for immunohistochemistry was obtained from Vector Laboratories (Burlingame, CA U.S.A.); the secondary peroxidase conjugate donkey anti-goat and anti-rabbit peroxidase conjugate were purchased from Santa Cruz Biotechnology (CA, U.S.A.) and from Sigma (St. Louis, MO, U.S.A.), respectively. For immunostaining the ABC Elite Vector Staining kit from Vector Laboratories was used. All chemicals were from Sigma. All the statistical analyses given in this paper were performed using ANOVA.

Isolation of RNA

MPS IIIB mice and age-matched normal animals, age 1, 3 and 7 months at the time of sacrifice, were killed with CO₂ and the brain and cerebellum were removed, subdivided into parts and immediately frozen in liquid nitrogen; total RNA was isolated from 50 mg of tissue using the RNeasy Lipid Tissue (Qiagen, MD U.S.A.) following the manufacturer's protocol. The concentration and purity of the RNA preparations were determined by measuring the absorbance at 260, 280 and 230 nm by spectrophotometer. Equal amounts of RNAs from at least three mice (normal or MPS IIIB) were then pooled before generating the cDNAs to

be used in the following experiments.

Microarray analysis

The GEArray™ Q series cDNA expression array filters (MM-002, MM-005, MM-010, MM-015) were used and hybridisation procedures were as described by the manufacturer. Briefly, the biotin dUTP-labeled cDNA probes were specifically generated using total RNA (5 µg per filter) from the 7-month-old mice and the AmpoLabeling-LPR kit. The array filters were then hybridized with biotin-labeled probes at 60° overnight. The membranes were then washed twice with 2 x saline sodium citrate buffer (SSC)/1% sodium dodecyl sulfate (SDS) and then twice with 0.1 x SSC/0.5%SDS at 60° for 15 min each. Chemiluminescent detection steps were performed by subsequent incubation of the filters with alkaline phosphate-conjugate streptavidine and CDP-Star substrate. All chemicals were from SuperArray Inc (MD, U.S.A.). All cDNA microarray experiments were performed twice and the data were analysed using the free software Scanalyze from Michael Eisen followed by the SuperArray GEArray Analyzer software.

Immunostaining

Before dissecting the brain, wild type and homozygous mutant mice at 7 months of age were anesthetised then perfused through the left ventricle with PBS pH 7.4 followed by 10% neutral buffered formalin solution; the brain was removed and fixed in formalin overnight at 4°C and embedded in paraffin. Sections were preincubated sequentially for 20 min with proteinase K 5 µg/ml, 5 min with 3% H₂O₂, and 30 min with BSA 1%; they were then reacted overnight with rabbit anti-caspase11 antibody (2µg/ml). For visualization by light microscopy, the sections

were reacted for 1 hour with secondary antibody conjugate to biotin (1:100). Colour was developed using diaminobenzidine (DAB) as chromogen (Vector Laboratories). To assess the number of Caspase 11 positive cells in sections, an area of 0.6 mm² was counted; at least twelve slices, six fields each, were stained and counted for each mouse and the mean is given for the number of positive cells per square millimeter.

In situ apoptosis detection

The terminal deoxynucleotidyl transferase-mediated dUTP nick end labeling (Tunel) method was used for detection of apoptotic cells using kit S7101 Chemicon (Temecula, CA), according to the manufacturer's instructions. Sections from brains of MPS IIIB and normal mice at 7 months of age were deparaffinised, rehydrated, and pretreated with proteinase K 20 µg/ml in PBS for 15 min. After blocking for endogenous peroxidase activity with 3% H₂O₂ in PBS, the sections were treated with equilibration buffer and incubated with terminal deoxynucleotidyl transferase enzyme at 37° for 1 h. The sections were then incubated with anti-digoxygenin conjugate to peroxidase and reacted with diaminobenzidine. The sections were counterstained with methyl green. Tunel-positive cells were counted in areas of 0.6 mm²; at least twelve slices, six fields each, were counted for each mouse and the mean is given for the number of positive cells per square millimeter.

RT-PCR

The cDNA was synthesized using 6 µg total RNA in the presence of random primers, dNTPs, RNase Inhibitor and Reverse Transcriptase (all from Promega, Madison WI U.S.A.) following the manufacturer's

protocol. The PCR was performed in 25 μ l reaction solution containing 12.5 μ l RT² Real-Time SYBR Green/ Fluorescein PCR Master Mix (from SuperArray Inc.), 1.0 μ l of template cDNA and 0.2 μ M PCR Primer set. The PCR conditions were as follows: 95°C 15 min, 40 cycles of 95°C for 30 s, 55°C for 30s, and 72°C for 5 min. Relative expression of mRNA for the target genes was performed by the comparative C_T ($\Delta\Delta$ C_T) method using the Abl gene as the control. A validation experiment was performed for each gene of interest and its control to determine the conditions for optimal concentration of primers and probes. The normalized C_T (Δ C_T) was obtained by subtraction of the C_T for Abl from the C_T for gene of interest. The difference between the Δ C_T for mutant and control samples gave rise to the $\Delta\Delta$ C_T value that was used for the calculation of the relative mRNA expression using the formula $2^{-\Delta\Delta C_T}$. The relative mRNA levels were expressed as fold change in MPS IIIB mice over control mice. The following primer pairs were used for each gene of interest: Abl (NM_009564), forward primer: 5'-GGTATGAAGGG AGGGTGTACCA-3', reverse primer: 5'-GTGAACTAACTCAGCCAGAGTGTTGA-3'; Cbln1, forward primer: 5'-TGCACACTCCCGTTTCCAA-3', reverse primer: 5'-TGGACGTGGGTAAGGAACCA-3'; BDNF, forward primer: 5'-ACACTGAGTCTCC AGGACAGCA-3', reverse primer: 5'-ATGCAACCGAAGTATGAAATAACCA-3'; Ccl3, forward primer: 5'-TGACACTCTGCAACCAAGTCTTC-3', reverse primer: 5'-AACGATGAATTG GCGTGGAA-3'; Casp11, forward primer: 5'-CTGATGCTGTCAAGCTGAGCC-3', reverse primer: 5'-TGACAAGAGCAAGCATGTTTCC-3'; gp91^{phox} (NM_007807), forward primer: 5'-GGAGTTCCAAG ATGCCTGGA-3', reverse

primer: 5'-CCACTAACATCACCCACCTCATAGC-3'; p47^{phox}
(NM_010876), forward primer: 5'-CCCAACTACGCAGGTGAACC-3',
reverse primer: 5'-AGCCGGTGATATCCCCTTTC-3'; p67^{phox}
(NM_010877), forward primer: 5'-GGCCTTCACCAAAA GCATCA-3',
reverse primer: 5'-GTCTATCAGCTGGTTCCCACG-3'; iNOS
(NM_010927), forward primer: 5'-GAGCAACTACTGCTGGTGGTGA-
3', reverse primer: 5'-GAGGGTACATGCTGGAGCCA-3'. All the
primers were designed by Primer Express software (Applied Biosystems,
CA, U.S.A.).

Western blot analysis

The presence of gp91^{phox} and BDNF in the brain and cerebellum of MPS IIIB and normal mice at 7 months of age was assessed by Western blot analysis. Fifty mg of tissues from three mice (normal or MPS IIIB) were pooled before homogenization. Total protein extracts were obtained by homogenization in Ripa lysis buffer with a mixture of protease inhibitors (both from Santa Cruz Biotechnology); protein concentration was measured and 50 µg of protein of each sample was electrophoresed by SDS-PAGE (7.5% gel for gp91^{phox} and 12.5% gel for BDNF). Proteins were then blotted on nitrocellulose membrane; the blocked membranes were incubated with antibodies against gp91^{phox} (goat,1:200) or BDNF (rabbit,1:500). After extensive washing with TBST the membranes were incubated with horseradish peroxidase-conjugate anti-goat or anti-rabbit secondary antibodies, and the bound antibodies were detected by Western blot luminol reagent (Santa Cruz Biotechnology).

Analysis of NADPH Oxidase Activity

NADPH oxidase activity was measured using a chemiluminescence detection system in homogenates prepared in phosphate buffer 100 mM, pH 7, by pooling brains or cerebella from MPS IIIB or normal 7-month-old mice (n=3). In these assays, 150 µg of proteins were added to a mix containing 50µM lucigenin, 50 mM phosphate buffer, 1mM EGTA, 150 mM sucrose, 0.1 mM NADH, 0.1 mM NADPH. Reactions were started by adding the proteins, and the production of superoxide ion was measured every 10 sec for 15 min by monitoring chemiluminescence using a luminometer Turner Biosystems 20/20ⁿ. The data, collected as relative luminescence units, were plotted versus time, and the area under the curve was used for analysis.

Results

Gene expression profile in the brain at 7 months from birth: microarray analysis

GEArray™ Q series cDNA expression filters were used as a first step for the analysis of gene expression. These membrane filters contained sequence verified gene fragments that used regions of cDNA selected to minimize potential cross-reactivity with related genes and for overall similarity in hybridization conditions. On the filter, each gene is reproduced in quadruplicate and controls (two house-keeping genes, *b-actin* and *GAPDH*, one negative control, two positive controls and blanks) are spotted across the base of the membrane, allowing a rapid assessment of the evenness of hybridization and straightforward quantitation and normalization on the same array (Fig. 3). The brains were collected from 7-month-old MPS IIIB and age-matched normal mice and RNA was isolated for the microarray analysis. A total of 355 genes present on 4 different membranes were assessed; the genes chosen were classified into four categories: genes related to apoptosis, genes for neurotrophins and receptors, genes for extracellular matrix (ECM) molecules and genes for chemokines, cytokines and their receptors. Of the genes tested, the expression of 274 transcripts was revealed in the 7-month-old mice, representing about 77% of all the genes examined. Of the expressed genes only those with a fold change ≥ 1.5 were considered significantly altered and therefore reported in Tab. 2. The microarray analysis showed that for the MPS IIIB mice 56 of the 274 genes examined were altered (i.e. approximately 20%) and the number of the upregulated transcripts (57%) was comparable to that of the

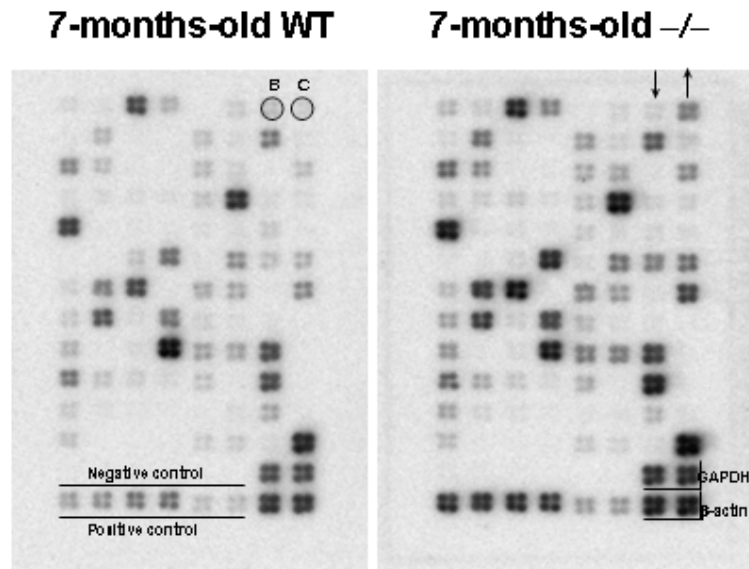


Fig. 3: Image profile of a representative cDNA filter array
 Brains from 7-months-old MPS IIIB (-/-) or normal mice (wt) (n=3) were dissected and the total RNA extraction was performed. Equal amounts of RNA from each mouse were then pooled before generating the cDNAs. cDNAs were used for hybridization to the neurotrophins and receptors microarray as described under materials and methods. Genes expressed in the affected brain (right panel) were identified as a specific hybridization signal and compared to the normal control (left panel). In addition to the test genes, each filter contained one negative control (PUC 18), two positive controls (Ppia and Rpl13a) and two house-keeping genes (β -actin and GAPDH) for normalization. Circles in the normal control delimit spots corresponding to representative genes found downregulated (B, Bdnf) or upregulated (C, Cbln1) in the 7-months -old MPS IIIB mice (arrows).

downregulated genes (43%). All but one the chemokines that were altered belonged to the group of transcripts present at a significantly higher level in the brain of the MPS IIIB mice than in the brain of the control mice, the only exception being the macrophage migration inhibitor factor (Mif), which presented a 0.66-fold change in its expression (Tab. 2). In these mice, most of the altered genes among the neurotrophins and their receptors were also upregulated, representing 77% of the members of this group. Conversely, all 17 ECM and adhesion molecules that were altered at 7 months from birth were expressed at significantly lower levels than in the control mice, with the exception of Col18A1 and CD44 (Tab. 2). Finally, a more balanced profile was exhibited by the apoptosis-related genes, 45% being upregulated and 55% showing a decreased expression in the MPS IIIB animals (Tab. 2).

Validation of the array analysis: real time RT PCR analysis on deregulated genes from the brain and cerebellum at 1, 3 and 7 months from birth

To confirm the gene expression pattern, some genes were selected and their expression analysed by real time RT-PCR on RNA extracts from 1-, 3- and 7-month-old mice. The genes, chosen on the basis of the results obtained from the array analysis, were: Bdnf and Cbln1, the genes most differentially expressed among the neurotrophin and receptor-related genes; Ccl3, the transcript with the highest expression among all the genes examined; Casp11 (Casp4) was chosen because it was recently reported to be an essential molecule in an apoptotic pathway of activated astrocytes (Suk et al, 2002).

Table 2. Array analysis: genes found deregulated in brains from 7 months-old MPS IIIB mice

| <u>Genebank accession n.</u> | <u>Gene symbol</u> | <u>Gene name</u> | <u>Fold chane</u> |
|--|-----------------------|--|-------------------|
| Chemokines, cytokines and receptors | | | |
| NM_011337 | Ccl3 (MIP-1 alpha) | chemokine (C-C motif) ligand 3 | 5.77 |
| NM_013652 | Ccl4 (MIP-1 beta) | chemokine (C-C motif) ligand 4 | 1.54 |
| NM_011332 | Ccl17 (Scya17) | chemokine (C-C motif) ligand 17 | 1.82 |
| NM_011888 | Ccl19 (Scya19) | chemokine (C-C motif) ligand 19 | 2.22 |
| U51717 | Ccr2 (MIP-1 alphaR) | chemokine (C-C motif) receptor 2 | 2.21 |
| NM_009916 | Ccr4 (Cmkbr4) | chemokine (C-C motif) receptor 4 | 2.50 |
| NM_007719 | Ccr7 (Cmkbr7) | chemokine (C-C motif) receptor 7 | 1.54 |
| NM_007720 | Ccr8 (Cmkbr8) | chemokine (C-C motif) receptor 8 | 2.92 |
| NM_007721 | Ccr10 (Cmkbr9) | chemokine (C-C motif) receptor 10 | 3.03 |
| NM_011798 | Cxcr1 (<u>Xcr1</u>) | chemokine (C motif) receptor 1 | 3.44 |
| NM_009909 | Il8rb (CXCR2) | interleukin 8 receptor, beta | 3.53 |
| AF102269 | Cx3cr1 | chemokine (C-X3-C) receptor 1 | 3.33 |
| NM_010560 | Il6st (gp130) | interleukin 6 signal transducer | 1.50 |
| NM_010548 | Il10 | interleukin 10 | 1.68 |
| NM_013584 | Lifr | leukemia inhibitory factor receptor | 2.08 |
| NM_010798 | Mif | macrophage migration inhibitory factor | 0.66 |
| NM_008907 | Ppia (CypA) | peptidylprolyl isomerase A | 1.75 |
| Neurotrophins and receptors | | | |
| NM_007540 | Bdnf | brain derived neurotrophic factor | 0.51 |
| NM_019626 | Cbln1 | cerebellin 1 precursor protein | 3.54 |
| NM_053007 | Cntf | ciliary neurotrophic factor | 2.00 |
| NM_011808 | Ets1 | E26 avian leukemia oncogene 1, 5' domain | 1.74 |
| M33760 | Fgfr1 | fibroblast growth factor receptor 1 | 1.93 |
| NM_139149 | Fus | fusion, derived from t(12;16) | 1.85 |

| | | | |
|------------------|--------------|---|------|
| | | malignant liposarcoma (human) | |
| NM_008115 | Gfra2 | glial cell line derived neurotrophic factor family receptor alpha 2 | 1.65 |
| NM_019791 | Maged1 | melanoma antigen, family D, 1 | 1.91 |
| NM_019548 | Tro (Maged3) | trophinin | 1.56 |
| NM_009750 | Ngfrap1 | nerve growth factor receptor (TNFRSF16) associated protein 1 | 1.54 |
| NM_008703 | Nmbr | neuromedin B receptor | 1.67 |
| NM_031199 | Tgfa | transforming growth factor alpha | 0.65 |
| NM_00103938 5 | Vgf | VGF nerve growth factor inducible | 0.52 |

| Extracellular matrix and adhesion molecules | | | |
|--|-----------------|---|------|
| NM_009818 | Catna1 | catenin (cadherin associated protein), alpha 1 | 0.68 |
| NM_018761 | Catn1l | catenin (cadherin associated protein), alpha-like 1 | 0.64 |
| X06340 | Cdh3 | cadherin 3 | 0.62 |
| NM_009867 | Cdh4 | cadherin 4 | 0.58 |
| NM_009929 | Col18A1 | procollagen, type XVIII, alpha 1 | 1.88 |
| M27130 | CD44 | CD44 antigen | 1.88 |
| NM_007899 | Ecm1 | extracellular matrix protein 1 | 0.61 |
| M18194 | Fn1 | fibronectin 1 | 0.52 |
| NM_016780 | Itgb3 (CD61) | integrin beta 3 | 0.56 |
| NM_021359 | Itgb6 | integrin beta 6 | 0.42 |
| NM_008482 | Lamb1 | laminin B1 subunit 1 | 0.53 |
| NM_008609 | Mmp15 (MT2-MMP) | matrix metalloproteinase 15 | 0.52 |
| NM_013903 | Mmp20 | Matrix metalloproteinase 20 | 0.53 |
| NM_010808 | Mmp24 (MT5-MMP) | matrix metalloproteinase 24 | 0.60 |
| NM_010810 | Mmp7 | matrix metalloproteinase 7 | 0.60 |
| NM_011346 | Sell | selectin, lymphocyte | 0.56 |
| NM_011581 | Thbs2 | thrombospondin 2 | 0.59 |
| Apoptosis-related genes | | | |
| NM_009684 | Apaf1 | apoptotic peptidase activating factor 1 | 1.90 |

| | | | |
|-----------|------------------|---|------|
| NM_009741 | Bcl2 | B-cell leukemia/lymphoma 2 | 0.58 |
| NM_007544 | Bid | BH3 interacting domain death agonist | 0.57 |
| NM_007609 | Casp11 (Casp4) | caspase 11, apoptosis-related cysteine peptidase | 1.95 |
| NM_007465 | Birc2 (IAP2) | baculoviral IAP repeat-containing 2 | 0.57 |
| NM_009403 | Tnfsf8 (Cd30l) | tumor necrosis factor (ligand) superfamily, member 8 | 0.62 |
| NM_011609 | Tnfrsf1a (Tnfr1) | tumor necrosis factor receptor superfamily, member 1a | 1.44 |
| NM_011610 | Tnfrsf1b (Tnfr2) | tumor necrosis factor receptor superfamily, member 1b | 0.56 |
| NM_011632 | Traf 3 | Tnf receptor-associated factor 3 | 1.50 |

Array analyses were performed on pooled RNA from ≥ 4 seven months-old MPS IIIB mice or age-matched controls.

The results of the real time analysis performed both for the brain and cerebellum of the mice are shown in Fig. 4. *Cbln1*, which was found by the array filters to be upregulated in the brain of the 7-month-old MPS IIIB mice was by real time PCR approximately 2.6- and 2.2-fold more expressed in the 3-month-old and 7-month-old MPS IIIB mice, respectively compared to the age matched normal controls, while remaining unchanged in the 1-month-old mice (Fig. 3 and Fig. 4, panel A). Conversely, the same gene was unaltered in the cerebellum of the MPS IIIB mice at all time points from birth (Fig. 4, panel B).

Also *Bdnf* was unchanged at 1 month from birth, both in the brain and cerebellum, but presented changes in the older mice. In the brain, it showed, a decreased expression (0.615 and 0.59 fold at 3 months and 7 months from birth, respectively) (Fig. 4, panel A), thus confirming the results provided by the arrays (Tab. 2); in the cerebellum, *Bdnf* presented different rates: it was downregulated in the 3-month-old MPS IIIB mice (0.3 fold) and upregulated in the older animals (2.22 fold) (Fig. 4, panel B). The results from the real time analysis were confirmed, for *Bdnf*, also at the protein level by Western blot (Fig. 4, panel C): as revealed by the densitometric analysis, the *Bdnf* polypeptide present in the homogenates from brains from the 7-month-old MPS IIIB mice was approximately one half compared to the normal controls (Fig. 4, panel C); conversely, a two-fold increase in the *Bdnf* protein level was seen in the cerebellum of the same animals (Fig. 4, panel C).

According to the array data, *Ccl3* proved to be the most upregulated gene in the brain of the MPS IIIB mice at every time point from birth: 9.65 fold at 1 month, 9.2 fold at 3 months and 11.4 fold at 7 months. Upregulation was confirmed also for *Casp11*: 7.62 fold at 1

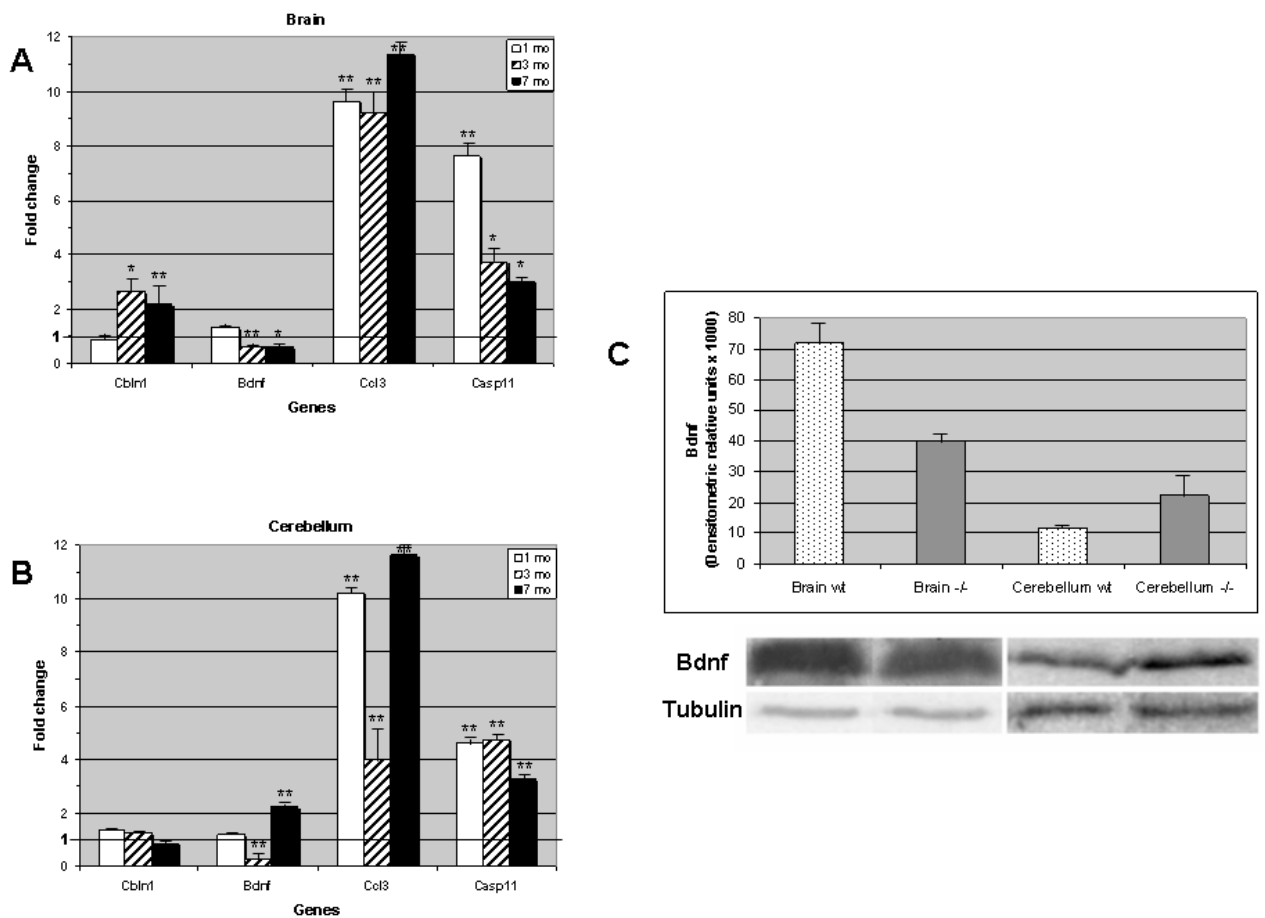


Fig. 4: Relative levels of Cbln1, Bdnf, Ccl3 and Casp11 in brain or cerebellum of affected mice.

Panels A and B: results from real time analysis performed on RNAs obtained from brains (panel A) or cerebella (panel B) dissected at different times from birth (n=4). Equal amounts of RNAs from each mouse were pooled before generating the cDNAs. Abl cDNA were used to normalize the level of gene of interest in both mutant and control preparations. Data (mean \pm SEM of three experiments performed in triplicate) are expressed as fold change in the affected mice compared to the normal control. White bars: 1-month-old mice; striped bars: 3-months-old mice; black bars: 7-months-old mice. *P<0.05; **P<0.001.

Panel C: western blot analysis of Bdnf levels in brain or cerebellum obtained from 7-months-old MPS IIIB (-/-, gray bars) or normal mice (wt, dotted bars) (n=3) and pooled before homogeneization. Histograms shown the values (mean \pm SEM of three experiments, P<0.05) obtained by densitometric analysis of Bdnf band normalized for tubulin levels. On the bottom: the western blot image refers to a representative experiment.

month, 3.73 fold at 3 months and 3.03 fold at 7 months from birth (Fig. 4, panel A). The same genes were always expressed at significantly higher levels than the normal controls also in the cerebellum (Fig. 4, panel B).

Immunohistochemistry and Tunel analysis

To verify whether the upregulation of Casp11 transcript resulted in identifiable immunoreactivity in the brain sections, we performed immunohistochemistry on paraffin sections from a 7-month-old MPS IIIB mouse and an age-matched normal control. Immunohistochemical staining with an anti-caspase 11 antibody demonstrated a response of positive cells in the brain, especially in the subcortical region (Fig. 5, panel B); the number of caspase-11 positive cells in the MPS IIIB mouse was approximately 2-fold the values for the control animal (Fig. 5, panel E). These results were in agreement with the Tunel analysis in which positive staining in the MPS IIIB mouse (Fig. 5, panel D) revealed a marked increase in apoptotic cells of 56-fold compared to the normal control (Fig. 5, panel F).

Candidate genes with potentially critical roles in CNS degeneration: the NADPH-dependent oxidase complex

Another set of genes to be analysed by real time RT PCR was selected on the basis of their potential role in the neurodegeneration; specifically, we chose to verify the expression of some components of

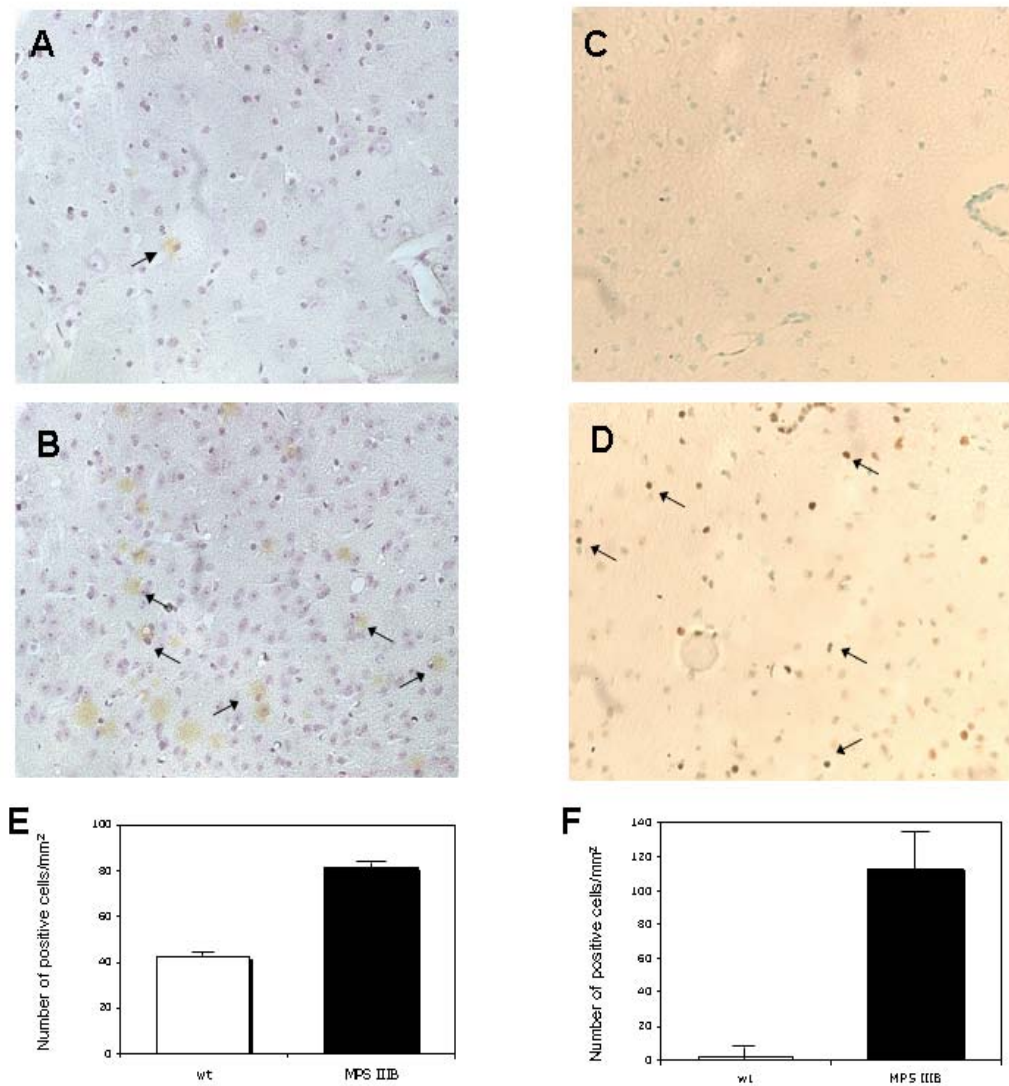


Fig. 5: Immunohistochemistry and TUNEL analysis on brain from 7-months-old mice.

Brain sections of 7 μ m were obtained from affected and normal mice at 7 months from birth. Panel A and B: brain sections stained with antibody against caspase-11 as described under Materials and Methods; arrows point to caspase 11 positive cells as resulting from peroxidase staining in the control (A) and in the MPS IIIB affected mouse (B). The slides were counterstained with hematoxylin. Magnification 40X.

Panels C and D: TUNEL staining on the affected mouse (D) compared to the normal age-matched control (C); arrows point to apoptotic cells. Magnification 40X.

Panels E and F: counts of caspase-11 positive cells (Panel E: $P < 0.05$) and TUNEL-positive cells (Panel F: $P < 0.0001$) in MPS IIIB mouse (-/-, black bars) compared to normal mouse (wt, white bars). At least twelve slices were stained and counted for each mouse and the mean (\pm SEM) is given for number of positive cells per square millimeter area.

the phagocytic NADPH-dependent oxidase enzyme complex, gp91^{phox}, p67^{phox} and p47^{phox}, to reveal a possible overproduction of superoxide ion that might be involved in the neuropathogenesis of MPS IIIB disease. For this reason, we also analysed the iNOS (inducible NO synthase) gene: it was recently suggested that the activation of microglial NADPH oxidase can be synergistic with glial iNOS expression in inducing neuronal death (Mander and Brown, 2005).

The real time analysis also on this second set of genes was performed on 1-, 3- and 7-month-old mice, both on the brain and cerebellum. The results from this analysis are reported in Fig. 6. As shown, gp91^{phox}, p67^{phox} and p47^{phox} were upregulated, both in the brain and cerebellum. The levels of the gp91^{phox} transcripts in the MPS IIIB mice was always at least three times higher than in the normal controls at each time point from birth, either in the brain or in the cerebellum (Fig. 6 panels A and B). For this gene the correspondence between the transcript levels and the protein levels was verified by Western blot analysis. As resulted from the densitometric analysis, approximately a three-fold increase in the gp91^{phox} protein level was evident in the 7-month-old MPS IIIB mice, both in the brain and cerebellum (Fig. 6, panel C). The p67 and p47 expression proved to be more variable, with the lowest values seen at 3 months from birth, both in the brain and cerebellum, but always higher than the normal controls (Fig. 6, panels A and B). Finally, the iNOS gene was also upregulated in the 1-month-old MPS IIIB mice, both in the brain (Fig. 6, panel A) and cerebellum (Fig. 6, panel B) but its expression reverted to normal levels in both organs from 3 months of age (Fig. 6, panels A and B).

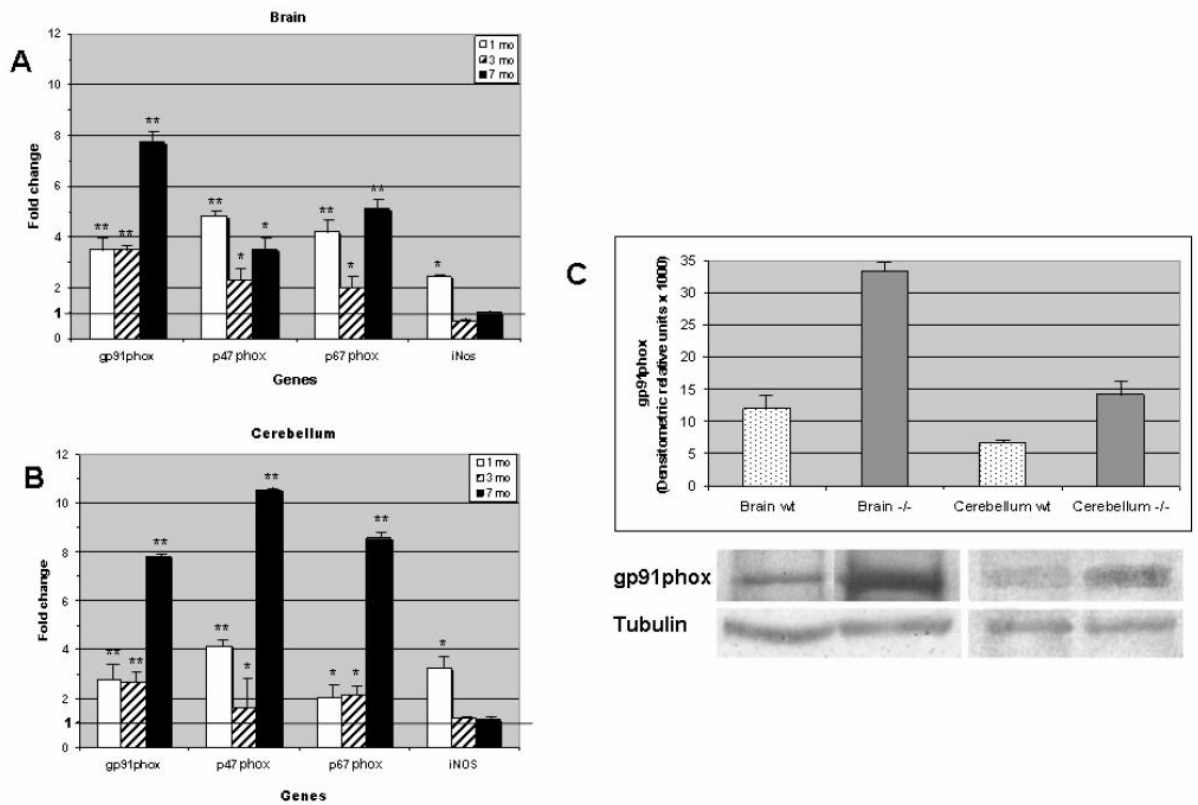


FIG. 6: Relative levels of gp91^{phox}, p47^{phox}, p67^{phox}, and iNOS in brain or cerebellum of affected mice.

Panels A and B: results from real time analysis performed on RNAs obtained from brains (panel A) or cerebella (panel B) dissected (n=4) at different times from birth. Equal amounts of RNAs from each mouse were pooled before generating the cDNAs. Abl cDNA were used to normalize the level of gene of interest in both mutant and control preparations. Data (mean ± SEM of three experiments performed in triplicate) are expressed as fold change in the affected mice compared to the normal controls. White bars: 1-month-old mice; striped bars: 3-months-old mice; black bars: 7-months-old mice. *P<0.05; **P<0.001.

Panel C: western blot analysis of gp91^{phox} levels in brain or cerebellum obtained from 7-months-old MPS IIIB (-/-, gray bars) or normal mice (wt, dotted bars)) (n=3) and pooled before homogenization. Histograms show the values (mean ± SEM of three experiments, P<0.05) obtained by densitometric analysis of gp91^{phox} band normalized for tubulin levels. On the bottom: the western blot image refers to a representative experiment.

To verify that the increased levels observed in the components of the NADPH oxidase resulted in an increased production of superoxide ion in the organs of the MPS IIIB mice, we determined the oxidase activity in the brain and cerebellum homogenates from 7-month-old mice. As seen in Fig. 6, the comparison between MPS IIIB and normal age-matched animals showed an approximately two-fold and three-fold increase in the chemiluminescence observed in the brain and cerebellum homogenates from the MPS IIIB mice, respectively. In all cases chemiluminescence was suppressed by SOD 30 U/ml, indicating that the main reactive oxygen species detected in the reaction was the superoxide ion (Fig. 7).

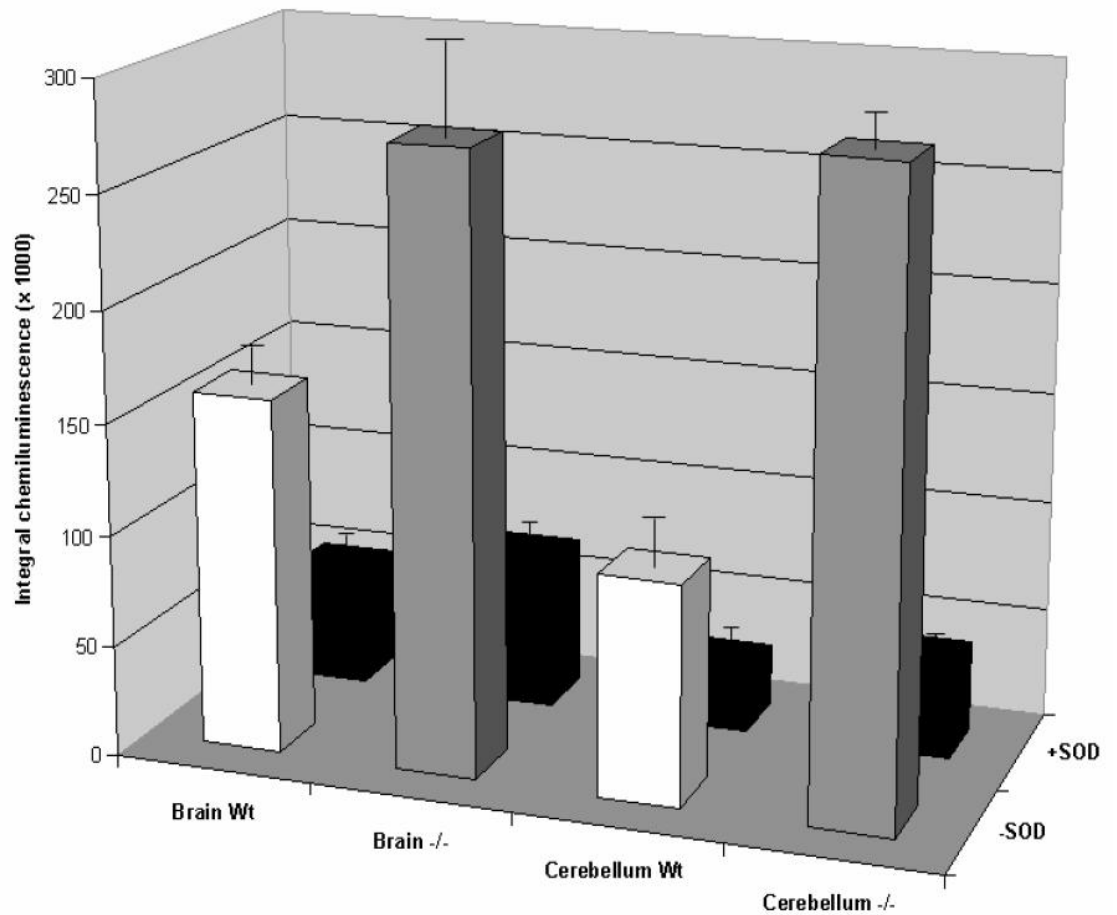


Fig. 7: Functional analysis of normal and mutant homogenates from 7-months-old mice in NADPH oxidase assay.

NADPH oxidase activity was determined in brains and cerebella homogenates, prepared pooling tissues from 7-months-old normal (wt, white bars) and affected (-/-, black bars) mice (n=3), by a lucigenin-based assay performed as described under Materials and Methods. Reaction were started by adding the proteins and the production of superoxide ion was measured each 10sec for 15 min by monitoring chemiluminescence. The data, collected as relative luminescence units, were plotted versus time, and the area under the chemiluminescence intensity curve (integral chemiluminescence) was used for analysis. The chemiluminescence was suppressed by superoxide dismutase (SOD) 30U/ml, indicating that the main reactive oxygen species detected in the reaction was the superoxide ion. Values are mean \pm SEM of three experiments (P<0.01).

Discussion

A variety of inter- and intracellular pathways have been described that underlie both pathologic and neuroprotective processes. Specifically, the studies characterizing the involvement of neurotrophins (Dawbarn and Allen, 2003), apoptosis-related pathways (Krantic et al., 2005) and inflammation mechanisms (Griffin, 2006) have revealed a great deal about the determinants of neuronal vulnerability.

Several genes involved in astrogliosis showed an increased expression in the brain of the MPS IIIB mice (Tab. 2). Brain inflammation, in fact, is characterized by reactive gliosis involving the activation of astrocytes and microglia. Gliosis, in turn, is associated to an increased production of cytokines and chronic activation of inflammatory pathways that take part in a large variety of phenomena occurring in brain disease, including neuronal cell damage, glial cell activation and proliferation, neurogenesis and alterations in the blood–brain barrier permeability, involving highly divergent diseases (for example, human immunodeficiency virus type-one associated dementia, Alzheimer's disease, Parkinson's disease, Sandhoff disease) (Kadiu et al, 2005, Wu and Proia, 2004). Among the chemokines, cytokines and receptors examined in the present study, all the altered genes except *Mif* were upregulated (Tab. 2). The early production of chemokines/cytokines occurs in resident microglia and astrocytes and is preceded by monocyte/macrophage recruitment. Particularly, *Ccl3* (MIP1-alpha) plays a pivotal role in macrophage recruitment, inducing monocytes to infiltrate the CNS and expanding the activated macrophage-microglial subpopulation. In the present study *Ccl3* was the most expressed chemokine from one month from birth, exhibiting the highest

upregulation among all the genes examined in the brain of the MPS IIIB mice. By real time analysis we demonstrated that Ccl3 was highly upregulated also in the cerebellum of the MPS IIIB mice. This chemokine was previously reported to be induced in the brain of a mouse model in another lysosomal storage disease, Sandhoff disease, from an early stage of the pathogenesis and to trigger an apoptosis of neurons, resulting in a rapid neurodegenerative course (Wu and Proia, 2004). Interestingly, we found another two related chemokines upregulated in the MPS IIIB brains: Ccl4 (MIP1-beta), a neutrophil survival factor that cooperates with Ccl3 for the neuronopathic effects induced by a murine oncornavirus (Askovic et al, 2001), and Ccr2, which was demonstrated to be involved in macrophage recruitment to the injured nervous system (Siebert et al, 2000), probably by establishing interaction with MCP-1 (1.34-fold increase in the MPS IIIB mice, data not shown), which at least in the liver, is required for optimal Ccl3 production, as recently reported (Hokeness et al, 2005).

The brain of MPS IIIB mice also showed at 7 months from birth increased levels of Il6st (gp130) and Lifr transcripts associated to a moderate increased expression of Il6 (1.24-fold compared to the normal controls, data not shown). Substantial evidence indicates that cytokines involved in the brain's response to injury include tumor necrosis factor, interleukin (Il)-1 and Il-6-type. In particular, a great deal of focus, has been put on the gp130 (Il-6-type) cytokines, a redundant and pleiotropic family of peptide signaling molecules that consists of at least six members including Il-6, leukemia inhibitory factor (Lif) and ciliary neurotrophic factor (Cntf) (Wang and Shuaib, 2002). All these cytokines share one or both of the receptor signal transducing subunits gp130 and

Lifr in their respective receptor complexes. They exert a variety of biological and cellular effects; among these, it has been suggested that they are also involved in the regulation of glial activation: for example, the induction of gp130-related cytokines and activation of the JAK2/STAT3 pathway in astrocytes precedes an up-regulation of glial fibrillary acidic protein in an experimental model of neurodegeneration (Sriram et al, 2004). In this respect, our result concerning the significant upregulation of Cntf in the brain of the MPS IIIB animals may be of particular interest. This gene is classified in Tab. 2 among the neurotrophins and receptors, since the protein encoded by it is a polypeptide hormone whose action appears to be restricted to the nervous system where it promotes neurotransmitter synthesis and neurite outgrowth in certain neuronal populations. However, there is substantial evidence that, in addition to its neurotrophic activity, Cntf regulates glial activation in the brain, and functions as an inducer of reactive gliosis. Cntf is strongly upregulated in activated astrocytes and the application of Cntf upregulates the GFAP expression in cultured astrocytes and induces various aspects of gliosis in the intact brain (Winter et al, 1995). The association between Cntf and its receptor, Cntfr, leads to recruitment and dimerization of gp130 and Lifr, both of which we found to be upregulated in the MPS IIIB brain, and these events in turn induce downstream signalling (Elson et al, 2000).

Finally, it is also interesting to note that in the MPS IIIB mice we found evidence of upregulation of CXCR2 receptor (Il8rb), which is an important neutrophil arrest chemokine *in vivo*, (Smith et al, 2004) and for the peptidyl prolyl isomerase A gene (Ppia, cyclophilin A), coding for a cytokine that activates endothelial cells and which was suggested as

playing an important role in the pathogenesis of inflammatory diseases (Jin et al, 2004). All the data reported above provide additional support for the major involvement of the inflammatory component in the brain pathogenesis of MPS IIIB disease.

Among the cytokines and chemokines examined the only downregulated gene in the brain of the MPS IIIB mice at 7 months from birth was the macrophage migration inhibitor factor (Mif). Mif exerts a critical proinflammatory action: its downregulation could be an integral component of a mechanism stimulating anti-inflammatory effects to defend the brain from chronic inflammation. The upregulation observed for Il10 could also be ascribed to this mechanism, since Interleukin-10 appears to be able to suppress microglial activation/macrophage infiltration and markedly reduces the production of proinflammatory cytokines by the activated microglia or macrophages (Stoeck et al, 2005).

The alterations observed for the neurotrophins and receptors in the brain of MPS IIIB mice include the interesting downregulation, demonstrated both at the RNA and protein level, of the brain derived neurotrophic factor (Bdnf). Bdnf, a secreted neurotrophin, regulates aspects of neuronal survival, migration, morphological and biochemical differentiation, and in adult life it plays a role in the maintenance of the neuronal phenotype and in the modulation of synaptic efficacy and plasticity. In particular, the hippocampus, which retains a high degree of plasticity and vulnerability throughout life, is one of the regions where Bdnf is expressed at high basal levels in the mature brain, where it is also required for the long-term survival of newborn neurons (Sarainen et al, 2005). The loss of Bdnf during the earlier stages of development causes hyperactivity and more pronounced hippocampal-dependent learning

deficits (Monteggia et al, 2004) as well as hippocampal-dependent memory impairment (Barrientos et al, 2003). In agreement with these data, it was reported that Bdnf is critical for the function and survival of neurons, which degenerate in the late stage of Alzheimer's disease (AD) and that the decrease in Bdnf precedes the decline in choline acetyltransferase activity occurring later in AD (Peng et al, 2005). Moreover, Bdnf, which is also synthesised by dopaminergic neurons in the adult nigrostriatal pathway, shows a significantly reduced expression in the Parkinson's disease substantia nigra and probably contributes directly to the death of nigral dopaminergic neurons and the development of Parkinson's disease (Porritt et al, 2005); decreased Bdnf expression was also observed in Huntington's disease, where it exacerbates dopaminergic neuronal dysfunction and participates in the motor disturbances associated with this neurodegenerative disorder (Pineda et al, 2005). Thus, the downregulation observed for Bdnf in the brain of the MPS IIIB mice seems to correlate well to the disturbance of the neuronal plasticity proposed for this murine model by Li et al (2002), as well as to the neurological clinical signs of the human disease, mainly hyperactivity and learning impairment. Such downregulation, however, appears to be a late molecular event in the pathogenesis of MPS IIIB-related brain disease, at least for the mouse model, since real time analysis revealed normal levels of Bdnf transcript in the one-month-old MPS IIIB animals and a downregulation from 3 months from birth. In addition the Bdnf levels in the cerebellum of the MPS IIIB mice proved to be more intricate since the real time analysis showed a transient decrease in the Bdnf transcripts at 3 months from birth, followed, surprisingly, by a consistent increase in its expression at 7 months from birth. We have no clear

explanation for this, but it is known that the cerebellum is a CNS region that is resistant to many neurodegenerative disorders such as stroke and Alzheimer's disease; this could be related to the recent findings suggesting that this region plays a vital role in learning, memory, fear conditioning, and cognitive processing (Wu et al, 2005). Thus, the cerebellum could have alternative mechanisms to induce protective levels of Bdnf, which by exerting a role as an essential factor for the maintenance of the cerebellar neural functions, could help to save part of the functionality of this organ.

Another interesting neurotrophin that was upregulated in the brain of the MPS IIIB mice was cerebellin 1 (Cbln). The Cbln1 gene codes for a cerebellin, a small polypeptide preferentially expressed in the cerebellum but also present at variable concentrations elsewhere in the CNS, especially in the hypothalamus. The precise function of cerebellin is controversial. However, recently it was reported that among midbrain populations of dopaminergic neurons cerebellin 1 is expressed in the A9 group in the substantia nigra 2.2-fold more than in the A10 neurons, and it is known that A9 cells are more vulnerable to factors causing neurodegeneration in Parkinson's disease (Chung et al, 2005); these observations suggest that Cbln1 may be involved in dopaminergic neuron survival/cell death and provide a possible link to the results shown above for Bdnf in MPS IIIB disease.

For the ECM-related molecules analysed in this study, it is noteworthy that several transcripts were altered in the MPS IIIB brains, mostly downregulated; this could result in possible alterations in the matrix and intracellular network integrity and contribute to the impairment of the neuronal functions. For example, we found decreased

levels of the α E-catenin (Catn1) transcript, and the central nervous system-specific deletion of this essential adherens junction gene was recently reported to cause abnormal activation of the hedgehog pathway, resulting in shortening of the cell cycle, decreased apoptosis and cortical hyperplasia (Lien et al, 2006). Matrix metalloproteinases (Mmps) have been said to remodel the extracellular environment of neurons and play crucial roles in regulating both normal and pathophysiological processes in the brain; among these, MT5-MMP (Mmp24), expressed in the neurons, and found by us to be downregulated in the MPS IIIB mice brain, plays an important role in axonal growth, which contributes to the regulation of the neural network formation and remodelling (Monea et al, 2006).

The results obtained from the analysis of the apoptosis-related genes are also intriguing. The decreased levels of the proapoptotic genes Bid and Tnfsf8 and the increased expression of the antiapoptotic gene Traf3 seem to suggest a limited involvement of apoptotic mechanisms in the brain pathology. However, the downregulation of the antiapoptotic genes Bcl2, Birc2 and Tnfr2, and the increased levels of the transcripts for Apaf1 (the core of the apoptosome in the intrinsic pathway for apoptosis), Tnfr1 and Casp11, apparently suggest apoptosis as a significant mechanism underlying the pathogenesis of the brain disease in the MPS IIIB murine model. In particular, for Casp11, for which the real time analysis confirmed the transcript upregulation, we also found evidence, by immunohistochemistry, of an increase in the corresponding polypeptide in the subcortical region of the MPS IIIB mouse brain; accordingly, the Tunel test showed, in the same region, a significant number of apoptotic cells. These results apparently disagree with a

previous report of an absence of neuronal cell apoptosis in the MPS IIIB mouse model (Li et al, 2002); however, it is possible that the Casp11 upregulation found in this study and the cell apoptosis observed can be primarily ascribed to the glial cells, as also suggested by the morphological analysis of the Casp11-positive cells. In effect, the apoptosis of activated astrocytes, mediated by caspase 11, was suggested as an autoregulatory mechanism for rat astrocyte activation (Suk et al, 2002), whereas mouse microglial cells undergo apoptosis upon inflammatory activation by an apoptotic pathway involving the induction of caspase 11 expression (Lee et al, 2001). Thus, the upregulation of Casp11 could be involved in the above hypothesized mechanism by stimulating anti-inflammatory effects to defend the brain from chronic inflammation. In this respect, also the upregulation of TRAF3 could contribute to limiting the inflammatory response since this molecule was recently reported to be essential for the induction of type I interferons and the anti-inflammatory Il-10, but dispensable for the expression of pro-inflammatory cytokines (Hacker et al, 2006). Moreover, it is interesting to note that also Bcl2 downregulation, as seen in the MPS IIIB mice, was suggested as a possible pathway involved in inflammatory activation-induced cell death (AICD) of glial cells (Suk et al, 2002).

Substantial evidence implicates the oxygen reactive species (ROS) in a variety of pathogenic events producing neurodegeneration. Indeed, ROS belong to the wide variety of factors that activate astrocytes and/or microglia and may mediate neuronal impairment; therefore we decided also to verify the expression in the MPS IIIB mice brain of some genes involved in the ROS production and not included in the set of genes analyzed by array. Specifically, we performed real time analysis for some

components of the phagocytic enzyme complex NADPH-dependent oxidase, gp91^{phox}, p67^{phox} and p47^{phox}. NADPH oxidase is the major source of ROS during inflammation, is expressed mainly by microglia and produces superoxide ion that can then be broken down mainly by extracellular and intracellular superoxide dismutase to give hydrogen peroxide. It is a multicomponent enzyme complex that includes an integral membrane heterodimer composed of gp91^{phox} and p22^{phox}, four cytosolic protein components, p47^{phox}, p67^{phox}, p40^{phox} and a small GTP-binding protein, Rac (Green et al, 2001). We demonstrate here that at least three components of this complex are upregulated, at the RNA and/or protein level, and, more importantly, that this leads to increased NADPH oxidase activity in the brains affected. It was recently reported that glial inducible nitric oxide synthase (iNOS) is induced in astrocytes and microglia by proinflammatory cytokines and that *in vitro* this increased expression is synergistic with the activation of microglial NADPH oxidase in inducing neuronal death by producing the neurotoxic peroxynitrite (Mander and Brown, 2005); therefore, we decided to verify whether this pathogenetic mechanism could be applied also to the MPS IIIB mouse model by performing real time analysis also on the glial iNOS. Interestingly, we observed a transient upregulation of the iNOS transcripts at one month from birth, followed by a normalization of the RNA levels at 3 and 7 months from birth. These data suggest that NADPH oxidase does not cause neurodegeneration via peroxynitrite in adult MPS IIIB mice; however it is possible that peroxynitrite is involved in neurodegeneration in the early stages of the pathogenesis. In any case, our finding that the MPS IIIB nervous tissues are able to overproduce superoxide ion and probably the related ROS could be important: ROS

could be involved in several ways in the neurodegenerative events underlying brain disease in MPS IIIB. For example, dopaminergic cell death seems to involve the production of microglia-derived proinflammatory factors, among which ROS, that might exceed proinflammatory cytokines (Wang et al, 2005); in particular, ROS overproduction could have a synergistic effect with the decrease observed in the Bdnf levels, since oxidative stress and neurotrophins deficiency seem to be factors triggering neurodegeneration in the substantia nigra (Onyango et al, 2005). It is also interesting that MCP-1/Ccl3 and Ppia expression and secretion appear to be influenced by oxidative stress (Nishi et al, 2005; Jin et al, 2004). Moreover, the increase in the NADPH oxidase activity in the MPS IIIB brain might also be linked to the upregulation of Ccr2 and CXCR2 observed, since Ccr2 deficiency attenuates oxidative stress (Hayasaki et al, 2006) while the activation of CXCR2 causes a translocation of Raf and Rac to the membrane fraction (Zhao et al, 2004).

Identifying the signaling mechanisms that modulate neuronal function during injury has important implications for understanding the pathophysiology of, and developing therapy for conditions that involve acute neuronal degeneration. Our findings further support the importance of inflammation, induced as a consequence of glial activation, in MPS III IIIB brain disease and provide insight on the possible involvement of oxidative stress in its pathogenesis.

References

1. Acarin, L., Gonzalez, B., Castellano, B., (2000) Neuronal, astroglial and microglial cytokine expression after an excitotoxic lesion in the immature rat brain. *Eur. J. Neurosci.* **12**:3505-3520.
2. Askovic, S., Favara, C., McAtee F. J., Portis, J.L., (2001) Increased expression of MIP-1 alpha and MIP-1 beta mRNAs in the brain correlates spatially and temporally with the spongiform neurodegeneration induced by a murine oncornavirus. *J. Virol.* **75** (6): 2665-74.
3. Barrientos, R. M., Sprunger, D.B., Campeau, S., Higgins, E.A., Watkins, L.R., Rudy, J.W., Maier, S.F. (2003) Brain-derived neurotrophic factor mRNA downregulation produced by social isolation is blocked by intrahippocampal interleukin-1 receptor antagonist. *Neuroscience***121**(4):847-53.
4. Beckman, J. S., Chen, J., Crow, J.P., Ye, Y.Z. (1994) Reactions of nitric oxide, superoxide and peroxynitrite with superoxide dismutase in neurodegeneration. *Prog. Brain Res.* **103**: 371-380.
5. Bhaumik, M., Muller, V.J., Rozaklis, T., Johnson, L., Dobrenis, K., Bhattacharyya, R., Wurzelmann, S., Finamore, P., Hopwood, J. J., Walkley, S. U., et al., (1999) A mouse model for mucopolysaccharidosis type III A (Sanfilippo syndrome). *Glycobiology*, **9**: 1389-1396.
6. Brickman, Y. G., Ford, M. D., Gallagher, J. T., Nurcombe, V., Bartlett, P. F., Turnbull, J. E. (1998) Structural modification of fibroblast growth factor-binding heparan sulfate at a determinative stage of neural development. *J. Biol. Chem.* **273**: 4350-4359.
7. Chung, C. Y., Seo, H., Sonntag, K.C., Brooks, A., Lin, L., Isacson, O. (2005) Cell type-specific gene expression of midbrain dopaminergic neurons reveals molecules involved in their vulnerability and protection. *Hum. Mol. Genet.* **14**(13): 1709-25.
8. Cressant, A., Desmaris, N., Verot, L., Brejot, T., Froissart, R., Vanier, M. T., Maire, I., Heard, J.M. (2004) Improved behavior and neuropathology in the mouse model of Sanfilippo type IIIB disease after adeno-associated virus-mediated gene transfer in the striatum. *Neurobiol. Dis.* **24** (45): 10229-10239.
9. Dahms, N. M., Iobele, P., Kornfeld, S. (1989) Mannose 6-Phosphate Receptors and lysosomal enzyme targeting. *J. Biol. Chem.* **264**, (21): 12115-12118.
10. Dawbarn, D., Allen, S. J. (2003) Neurotrophins and neurodegeneration. *Neuropathol. Appl. Neurobiol.* javascript:AL_get(this, 'jour', 'Neuropathol Appl Neurobiol. '); **29**(3):211-30.

11. Di Natale, P., Salvatore, D., Daniele, A., Bonatti, S. 1985 Biosynthesis of α -N-acetylglucosaminidase in cultured human kidney carcinoma cells. *Enzyme* **33**: 75-83.
12. Di Natale, P., Di Domenico, C., Gargiulo, N., Castaldo, S., Gonzalez Y Reyero, E., Mithbaokar, P., De Felice M., Follenzi, A., Naldini, L., Villani, G.R.D. (2005) Treatment of the mouse model of mucopolysaccharidosis type IIIB with lentiviral-NAGLU vector. *Biochem. J.* **388**: 639-646.
13. Ellinwood, N. M., Wang, P., Skeen, T., Sharp, N. J. H., Cesta, M., Decker, S., Edwards, N. J., Bublot, I., Thompson, J. N., Bush, W., Hardam, E., Haskins, M.E., Giger, U. (2003) A model of mucopolysaccharidosis IIIB (Sanfilippo syndrome type IIIB): N-acetyl- α -D-glucosaminidase deficiency in Schipperke dogs. *J. Inherit. Met., Dis.* **26** 489-504.
14. Elson, G. C., Lelievre, E., Guillet, C., Chevalier, S., Plun-Favreau, H., Froger, J., Suard, I., de Coignac, A. B., Delneste, Y., Bonnefoy, J. Y., Gauchat, J. F., Gascan, H. (2000) CLF associates with CLC to form a functional heteromeric ligand for the CNTF receptor complex. *Nat Neurosci* **3**(9):867-72.
15. Fischer, A., Carmichael, K. P., Munnell, J. F., Jhabvala, P., Thompson, J. N., Matalon, R., Jezyk, P. F., Wang, P. & Giger, U. (1998) Sulfamidase deficiency in a family of Dachshunds: a canine model of mucopolysaccharidosis IIIA. *Pediatr. Res.* **44**: 47-82.
16. Fu, H., Salmulski, R. J., McCown, T. J., Picornell, Y. J., Fletcher D., Muenzer, J. J. (2002) Neurological correction of lysosomal storage in a mucopolysaccharidosis IIIB mouse model by adeno-associated virus-mediated gene delivery. *Molec. Ther.* **5**: 42-49.
17. Gao, H.M., Liu, B., and Hong J.S. (2003) Critical Role for Microglial NADPH Oxidase in Rotenone-Induced Degeneration of Dopaminergic Neurons. *J. Neurosci.* **23** (15): 6181– 6187.
18. Giger, U., Shivaprasad, H., Wang, P., Jezyk, P., Patterson, D. & Bradley, G. (1997) Mucopolysaccharidosis type IIIB (Sanfilippo B syndrome) in emus. *Vet. Pathol.* **14**: 473 (Abstract).
19. Gomez-Pinilla, F., Vu, L., Cotman, C. W. (1995) Regulation of astrocyte proliferation by FGF-2 and heparan sulfate in vivo. *J. Neurosci.* **15**: 2021-2029.
20. Green, S. P., Cairns, B., Rae, J., Errett-Baroncini, C., Hongo, J. A., Erickson, R. W., Curnutte, J. T., (2001) Induction of gp91-phox, a components of the phagocyte NADPH oxidase, in microglial cells during central nervous system inflammation. *J. Cereb. Blood Flow Metab.* **21**: 374-384.

21. Griffin, W. S. (2006) Inflammation and neurodegenerative diseases. *Am. J. Clin. Nutr.* **83**(2): 470S-474S.
22. Hacker, H., Redecke, V., Blagoev, B., Kratchmarova, I., Hsu, L. C., Wang, G.G., Kamps, M. P., Raz, E., Wagner, H., Hacker, G., Mann, M., Karin, M. (2006) Specificity in Toll-like receptor signalling through distinct effector functions of TRAF3 and TRAF6. *Nature* **439**(7073): 204-7 Epub2005Nov23.
23. Hatten, M. E., Liem, R. K., Shelanski, M. L., Mason, C. A. (1991) Astroglia in CNS injury. *Glia* **4**: 233-243.
24. Hayasaki, T., Kaikita, K., Okuma, T., Yamamoto, E., Kuziel, W. A., Ogawa, H., Takeya, M. (2006) CC chemokine receptor-2 deficiency attenuates oxidative stress and infarct size caused by myocardial ischemia-reperfusion in mice. *Circ. J.* **70**(3): 342-51.
25. Hokeness, K. L., Kuziel, W. A., Biron, C. A., Salazar-Mather, T. P. (2005) Monocyte chemoattractant protein-1 and CCR2 interactions are required for IFN-alpha/beta-induced inflammatory responses and antiviral defense in liver. *J. Immunol.* **174**(3): 1549-56.
26. Ischiropoulos, H. and Beckman, J., S. (2003) Oxidative stress and nitration in neurodegeneration: Cause, effect, or association? *J. Clin. Invest.* **111**: 163-169.
27. Jin, Z. G., Lungu, A. O., Xie, L., Wang, M., Wong, C., Berk, B. C. (2004) Cyclophilin A is a proinflammatory cytokine that activates endothelial cells. *Arterioscler. Thromb. Vasc. Biol.* **24**(7):1186-91. Epub 2004 May 6.
28. Jones, M.Z., Alroy, J., Boyer, P., Cavanagh, K. T., Johnson, K., Gage, D., Vorro, J., Render, J. A., Common, R. S., Leedle, R. A., et al. (1998) Caprine mucopolysaccharidosis-IIID: clinical, biochemical, morphological and immunohistochemical characteristics. *J. Neuropathol. Exp. Neurol.* **57**: 148-157.
29. Kadiu, I., Glanzer, J. G., Kipnis, J., Gendelman, H. E., Thomas, M.P. (2005) Mononuclear phagocytes in the pathogenesis of neurodegenerative diseases. *Neurotox. Res.* **8**(1-2):25-50.
30. Krantic, S., Mechawar, N., Reix, S., Quirion, R. (2005) Molecular basis of programmed cell death involved in neurodegeneration. *Trends Neurosci.* **28**(12):670-6. Epub 2005 Oct 10.
31. Kurihara, M., Kumagai, K., Yagishita, S. (1996) Sanfilippo type C: a clinicopathological autopsy study of a long-term survivor. *Pediatr. Neurol.* **14**: 317-321.

32. Lee, J. Hur, J., Lee, P., Kim, J. Y., Cho, N., Kim, S. Y., Kim, H., Lee, M. S., Suk, K. (2001) Dual role of inflammatory stimuli in activation-induced cell death of mouse microglial cells. Initiation of two separate apoptotic pathways via induction of interferon regulatory factor-1 and caspase-11. *J Biol. Chem.* **276**(35):32956-65. Epub 2001 Jun 11.
33. Li, H.H., Yu, W.H., Rozengurt, N., Zhao, H.Z., Lyons, K. M., Anagnostaras, S., Fanselow, M., Suzuki, K., Vanier, M. T., Neufeld, E. F. (1999) Mouse model of Sanfilippo syndrome type B produced by targeted disruption of the gene encoding α -N-acetylglucosaminidase. *PNAS* **96** (25): 14505-14510.
34. Li, H.H., Zhao, H.Z., Neufeld, EF, Cai Y, Gomez-Pinilla F (2002) Attenuated plasticity in neurons and astrocytes in the mouse model of Sanfilippo syndrome type B. *J. Neurosci. Res.* **69**: 30-8.
35. Lien, W. H., Klezovitch, O., Fernandez, T. E., Delrow, J., Vasioukhin, V. (2006) α E-catenin controls cerebral cortical size by regulating the hedgehog signaling pathway *Science* **311**(5767):1609-12.
36. Mander, P., and Brown, G. C. (2005) Activation of microglial NADPH oxidase is synergistic with glial iNOS expression in inducing neuronal cell death: a dual-key mechanism of inflammatory neurodegeneration. *J. of Neuroinflammation* 2:20.
37. Monea, S., Jordan, B. A., Srivastava, S., DeSouza. S., Ziff, E. B. (2006) Membrane localization of membrane type 5 matrix metalloproteinase by AMPA receptor binding protein and cleavage of cadherins. *J Neurosci* **26**(8): 2300-12.
38. Monteggia, L. M., Barrot, M., Powell, C. M., Berton, O., Galanis, V., Gemelli, T., Meuth, S., Nagy, A., Greene, R. W., Nestler, E. J. (2004) Essential role of brain-derived neurotrophic factor in adult hippocampal function. *Proc. Natl. Acad. Sci. U S A* **101**(29):10827-32. Epub 2004 Jul 12.
39. Myerowitz, R., Lawson, D., Mizukami, H., Mi, Y., Tiffit, C., Proia, R. L. (2002) Molecular pathophysiology in Tay-Sachs and Sandhoff diseases as revealed by gene expression profiling. *Hum Mol Genet* **11** (11): 1343-1350.
40. Neufeld, E. F. & Muenzer, J. (2001) The mucopolysaccharidoses. In: Scriver CR, Beaudet AL, Sly WS, Valle D (eds), "The metabolic and molecular bases of inherited disease". 8th Ed New York: McGraw-Hill; pp. 3421-3452.
41. Nishi, T., Maier, C. M., Hayashi, T., Saito, A., Chan, P. H. (2005) Superoxide dismutase 1 overexpression reduces MCP-1 and MIP-1 alpha expression after transient focal cerebral ischemia. *J Cereb Blood Flow Metab* **25**(10): 1312-24.

42. Nurcombe, V., Ford, M. D., Wildschut, J. A., Bartlett, P. F. (1993) Developmental regulation of neural response to FGF-1 and FGF-2 by heparan sulfate proteoglycan. *Science* **260**: 103-106.
43. Ohmi, K., Greenberg, D.S., Rajavel, K.S., Ryazantsev, S., Li, H. H., Neufeld, E.F. (2003) Activated microglia in cortex of mouse models of mucopolysaccharidosis I and IIIB. *Proc. Nat. Acad. Sci. USA* **100**: 1902-1907.
44. Onyango, I. G., Tuttle, J. B., Bennett, J. P. Jr (2005) Brain-derived growth factor and glial cell line-derived growth factor use distinct intracellular signaling pathways to protect PD cybrids from H₂O₂-induced neuronal death. *Neurobiol. Dis.* **20**(1): 141-54.
45. Peng, S., Wu, J., Mufson, E. J., Fahnstock, M. (2005) Precursor form of brain-derived neurotrophic factor and mature brain-derived neurotrophic factor are decreased in the pre-clinical stages of Alzheimer's disease. *J. Neurochem.* **93**(6): 1412-21.
46. Pineda, J. R., Canals, J. M., Bosch, M., Adell, A., Mengod, G., Artigas, F., Ernfors, P., Alberch, J. (2005) Brain-derived neurotrophic factor modulates dopaminergic deficits in a transgenic mouse model of Huntington's disease. *J. Neurochem.* **93**(5): 1057-68.
47. Porritt, M. J., Batchelor, P. E., Howells, D. W. (2005) Inhibiting BDNF expression by antisense oligonucleotide infusion causes loss of nigral dopaminergic neurons. *Exp. Neurol.* **192**: 226– 234.
48. Rahmoune, H., Chen, H. L., Gallagher, J. T., Rudland, P. S., Fernig, D. G., (1998) Interaction of heparan sulfate from mammary cells with acidic fibroblast growth factor (FGF) and basic FGF. Regulation of the activity of basic FGF by high and low affinity binding sites in heparan sulfate. *J. Biol. Chem.* **273**: 7303-7310.
49. Ridet, J. L. Malhotra, S. K., Privat, A., Gage, F. H. (1997) Reactive astrocytes: cellular and molecular cues to biological function. *Trends Neurosci.* **20**: 570-577.
50. Rothstein, J. D., Dykes-Hoberg, M., Pardo, C. A., Bristol, L. A., Jin, L., Kuncl, R. W., Kanai, Y., Hediger, M. A., Wang, Y., Schielke, J. P., Welty, D. F. (1996) Knockout of glutamate transporters reveals a major role for astroglial transport in excitotoxicity and clearance of glutamate. *Neuron.* **16**: 675-686.
51. Ruoslahti, E., and Yamaguchi, Y. (1991) Proteoglycans as modulators of growth factor activities. *Cell* **64**: 867-869.

52. Sabatini, D.D., A.M.B. (2001) The Biogenesis of Membranes and Organelles. In Scriver, C.R., A.L. Beaudet, W.S. Sly, D. Valle, In *The Metabolic and Molecular Bases of Inherited Disease*, 8th ed. (Mc Graw-Hill, New York, USA) pp. 433-520.
53. Sahagian, G G., Distler, J., Jourdian, G. W. (1981) Characterization of a membrane-associated receptor from bovine liver that binds phosphomannosyl residues of bovine testicular β -galactosidase. *Proc. Natl. Acad. Sci. USA* javascript:AL_get(this, 'jour', 'Proc Natl Acad Sci U S A. '); **78**: 4289-4293.
54. Sairanen, M., Lucas, G., Ernfors, P., Castren, M., Castren, E. (2005) Brain-derived neurotrophic factor and antidepressant drugs have different but coordinated effects on neuronal turnover, proliferation, and survival in the adult dentate gyrus. *J. Neurosci.* **25**(5):1089-94.
55. Salvatore, D., Bonatti, S., Di Natale, P. (1984) Lysosomal α -N-acetylglucosaminidase: purification and characterisation of the human enzyme. *Bull. Mo.l Bio. Med.* **9**: 111-121.
56. Sasaki, T., Sukegawa, K., Masue, M., Fukuda, S., Tomatsu, S., Orii, T. (1991) Purification and partial characterisation of α -N-acetylglucosaminidase from human liver. *Biochem. J.* **110**: 842-846.
57. Siebert, H., Sachse, A., Kuziel, W. A., Maeda, N., Bruck, W. (2000) The receptor CCR2 is involved in macrophage recruitment to the injured peripheral nervous system. *J. Neuroimmunol.* **110**(1-2):177-85.
58. Smith, M. L. Olson, T. S., Ley, K. (2004) CXCR2- and E-selectin-induced neutrophil arrest during inflammation in vivo. *J. Exp. Med.* **200**(7):935-9.
59. Sriram, K., Benkovic, S. A., Hebert, M. A., Miller, D. B., O'Callaghan, J. P. (2004) Induction of gp130-related cytokines and activation of JAK2/STAT3 pathway in astrocytes precedes up-regulation of glial fibrillary acidic protein in the 1-methyl-4-phenyl-1,2,3,6-tetrahydropyridine model of neurodegeneration: key signaling pathway for astrogliosis in vivo? *J. Biol. Chem.* **279**(19):19936-47. Epub 2004 Mar 2.
60. Stoeck, K., Bodemer, M., Ciesielczyk, B., Meissner, B., Bartl, M., Heinemann, U., Zerr, I. (2005) Interleukin 4 and interleukin 10 levels are elevated in the cerebrospinal fluid of patients with Creutzfeldt-Jakob disease. *Arch. Neurol.* **62**(10):1591-4.
61. Suk, K., Kim, S. Y., Kim, H. (2002) Essential role of caspase-11 in activation-induced cell death of rat astrocytes. *J Neurochem* **80**(2):230-8.

62. Tamagawa, K., Morimatsu Y., Fujisawa, K., Hara, A., Taketomi, T., (1985) Neuropathological study and chemico-pathological correlation in sibling cases of Sanfilippo syndrome type B. *Brain Dev.* **7**: 599-609.
63. Tessitore, A., Villani, G.R.D., Di Domenico, C., Filocamo, M., Gatti, R., Di Natale, P. (2000) Molecular defects in the α -N-acetylglucosaminidase gene in Italian Sanfilippo type B patients. *Human. Genet.* **107**: 568-576.
64. von Figura, K., Hasilik, A., Steckel, F., van de Kamp, J.J. (1984) Biosynthesis and maturation of alpha-N-acetylglucosaminidase in normal and Sanfilippo B fibroblast. *Am. J. Hum. Genet.* **36**: 93-100.
65. Wang, C. X., Shuaib, A. (2002) Involvement of inflammatory cytokines in central nervous system injury. *Prog. Neurobiol.* **67**:161–172.
66. Wang, X., Chen, S., Ma, G., Ye. M., Lu, G.(2005) Involvement of proinflammatory factors, apoptosis, caspase-3 activation and Ca²⁺ disturbance in microglia activation-mediated dopaminergic cell degeneration. *Mech. Ageing. Dev.* **126**(12):1241-54. Epub 2005 Aug 19.
67. Weber, B., Blanch, L., Clements, P. R., Scott, H. S., Hopwood, J. J. (1996) Cloning and expression of the gene involved in Sanfilippo B syndrome (mucopolisaccharidosis III B). *Hum Mol genet* **5**: 771-777.
68. Weber, B., Hopwood, J. J., Yogalingam, G. (2001) Expression and characterisation of human recombinant α -N-acetylglucosaminidase. *Protein Express Purif.* **21**: 251-259.
69. Winter, C. G., Saotome, Y., Levison, S. W., Hirsh, D. (1995) A role for ciliary neurotrophic factor as an inducer of reactive gliosis, the glial response to central nervous system injury. *Proc. Natl. Acad. Sci. USA* **92**(13): 5865-9.
70. Wu, Y. P., Proia, R.L (2004) Deletion of macrophage-inflammatory protein 1a retards neurodegeneration in Sandoff disease mice. *Proc. Nat. Acad. Sci.* **101** (22): 8425-8430.
71. Wu, X., Jiang, X., Marini, A. M., Lipsky, R. H. (2005) Delineating and understanding cerebellar neuroprotective pathways: potential implication for protecting the cortex. *Ann. N. Y. Acad. Sci.* **1053**: 39-47.
72. Yogalingam, G., Weber, B., Meehan, J., Rogers, J., Hopwood, J.J. (2000) Mucopolysaccharidosis type IIIB: characterisation and expression of wild-type and mutant recombinant α -N-acetylglucosaminidase and relationship with Sanfilippo phenotype in an attenuated patient. *Biochim. Biophys Acta* **1502**: 415-425.

73. Yu, W.H., Zhao, K.W., Ryazantsev, S., Rozengurt, N., Neufeld, E.F. (2000) Short-term enzyme replacement in the murine model of Sanfilippo syndrome type B. *Mol. Gen. Metab.* **71**: 573-580.
74. Zhao, H.G., Li H. H., Schmidtchen, A., Bach, G., Neufeld, E. F. (1995) The gene encoding α -N-acetylglucosaminidase and mutations underlying Sanfilippo B syndrome (abstract). *Am. J. Hum. Genet. Suppl.* **57**: A 185.
75. Zhao, H.G., Li H. H., Bach, G., Schmidtchen, A., Neufeld, E. F. (1996) The molecular basis of Sanfilippo B syndrome. *Proc. Natl. Acad. Sci. USA* **93**: 6101-6105.
76. Zhao, K. W., Neufeld, E. F. (2000) Purification and characterisation of recombinant human α -N-acetylglucosaminidase secreted by Chinese hamster ovary cells. *Protein Express Purif.* **19**: 202-211.
77. Zhao, Wimmer, A., Trieu, K., Discipio, R. G. Schraufstatter IU (2004) Arrestin regulates MAPK activation and prevents NADPH oxidase-dependent death of cells expressing CXCR2. *J. Biol. Chem.* **279**(47):49259-67. Epub 2004 Sep 13.
78. Zhu, X., Raina, A. K., Lee, H. G., Casadesus, G., Smith, M. A., Perry, G. (2004) Oxidative stress signalling in Alzheimer's disease. *Brain Res.* **1000**(1-2): 32-9.

|
|

Words of Gratitude

I'd like to thank Prof. Paola Di Natale for giving me the opportunity to perform these studies, for the suggestions and the enthusiasm with which she always supported my job. I express appreciation to Dr. Guglielmo Villaniand and Dr. Carmela Di Domenico for advices on technical problems.